Case Studies in Thermal Engineering 81 (2026) 108025

Contents lists available at ScienceDirect

Case Studies in Thermal Engineering

journal homepage: www.elsevier.com/locate/csite

Reduction of the HVAC system size in school buildings through Earth-to-Air Heat Exchangers (EAHE)

D. D'Agostino [a], N. Kouki [b], F. Minelli [a], F. Minichiello [a], A. Vityi [b,*]

[a] Department of Industrial Engineering, University of Naples Federico II, Naples, 80125, Italy
[b] Institute of Environmental Protection and Nature Conservation, Faculty of Forestry, University of Sopron, Sopron, 9400, Hungary

HIGHLIGHTS

- A new hybrid HVAC system with Earth-to-Air Heat Exchanger (EAHE) is proposed.
- The reduction of the design capacity of coils within air handling unit is assessed.
- The system cuts heating and cooling peak loads up to 72.9% and 76.8%, respectively.
- Optimal 0.2 m × 100 m layout of the EAHE achieved about 88% thermal effectiveness.
- Performance gains were confirmed in both Mediterranean and Continental climates.

GRAPHICAL ABSTRACT

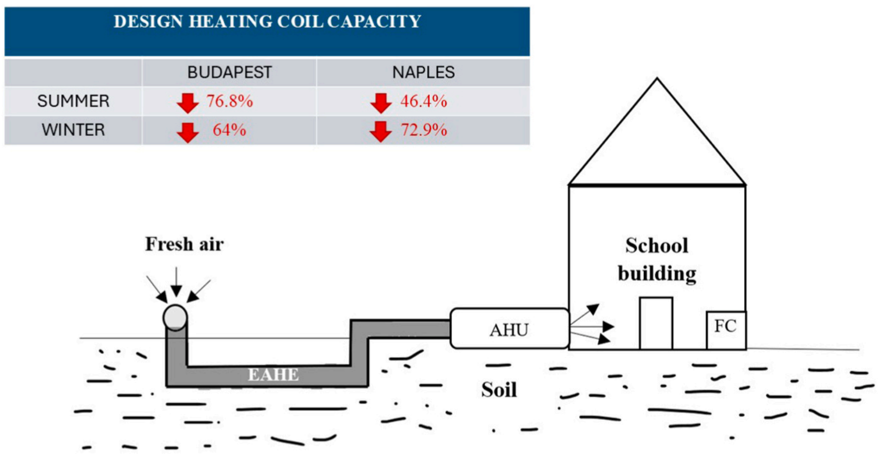

ARTICLE INFO

Keywords:
School building
EAHE
Geothermal energy
HVAC system
Sensitivity analyses
AHU

ABSTRACT

Aligned with the sustainability objectives promoted by the European Union, increasing attention is being directed toward improving the environmental performance of non-residential buildings, particularly schools, where indoor air quality and thermal comfort must be ensured while limiting energy consumption. This study investigates the integration of an Earth-to-Air Heat Exchanger (EAHE) into the Heating, Ventilation and Air-Conditioning (HVAC) system for an existing school building located in Southern Italy, with a comparative assessment under Mediterranean (Naples, Italy) and Continental (Budapest, Hungary) climate conditions. The building is equipped with fan-

* Corresponding author.
E-mail address: vityi.andrea@uni-sopron.hu (A. Vityi).

https://doi.org/10.1016/j.csite.2026.108025
Received 22 December 2025; Received in revised form 18 March 2026; Accepted 4 April 2026
Available online 4 April 2026

coil units and an Air Handling Unit (AHU). In the proposed configuration, the EAHE is positioned upstream of the AHU to pre-condition outdoor air by exploiting the relative thermal stability of the ground, thereby reducing the thermal capacity of the AHU coils. A parametric analysis was performed by varying pipe length and diameter to identify the optimal geometric configuration. The combination of a 0.2 m diameter and a 100 m pipe length proved to be optimal, achieving the highest thermal effectiveness ($\varepsilon \approx 88\%$) and the largest temperature difference between EAHE inlet and outlet air. With this configuration, the design heating coil capacity was reduced by up to 64% in Budapest and 72.9% in Naples during winter conditions. In summer conditions, the design cooling coil capacity decreased by 76.8% and 46.4%, respectively. The results demonstrate that the optimized EAHE configuration significantly reduces the thermal capacity of the AHU coils while enhancing the thermal stability of supply air, particularly in climates with pronounced seasonal variations.

1. Introduction

Currently, the building and industrial sectors contribute to around 39% and 31% [1] of the total global energy consumption, respectively. Particularly in building sector the consumption of energy related to electrical usage in households, that is approximately 40%, is linked to HVAC systems [2] and accounts for 36% of CO_2 emissions [3]. As a result, European strategies emphasize the importance of lowering energy consumption in HVAC systems by 11.7% and their CO_2 emissions by at least 55% compared to 1990 levels by 2030 [4], [5]. Additionally, climate changes directly impact electric energy production and consumption, water resources and agriculture. Above all, they influence the consumption of energy resources intended to heat and cool buildings [6]. Today, it is widely recognized that it is essential to identify solutions that concurrently promote sustainability, power efficiency and adaptation to climate change [7], [8], [9]. The "European Green Deal" [10] promotes the goal of attaining a climate-neutral Europe by 2050, focusing on the ambitious task of increasing the use of renewable energy and improving energy efficiency across all sectors [11]. While decarbonisation is essential across various sectors, there is a significant need for enhancement in operational energy efficiency of buildings [12], [13]. The increase in energy use within buildings has resulted in growing issues related to their environmental consequences [14].

Especially in school buildings, the indoor air quality (IAQ) is crucial, since children typically spend about 6-8 h each day in the school environment [15]. Globally, the target objective within these buildings is to provide a healthier interior environment by enhancing IAQ through the reduction or elimination of air pollution sources and the implementation of regulations or preventative measures [16]. To maintain optimal IAQ, the U.S. federal Environmental Protection Agency (EPA) [17] advises enhancing ventilation in these building.

There is an urgent need to swap to alternative energy sources rather than the conventional fuel or at least reduce its extensive use and resulting effects on the environment [18]. The term "alternative sources of energy" refers not only to efficient options but also to forms of clean and renewable energy [19], [20]. These sources are essentially inexhaustible and can be effectively exploited, like geothermal energy [21].

Today HVAC systems are usually based on vapor compression machines; however, global warming and the ozone layer depletion caused by chlorofluorocarbons (CFCs), along with the necessity to reduce the consumption of high-quality energy, has led to the exploration of various substitute techniques [22], [23]. One effective technique is the Earth–to-Air Heat Exchanger (EAHE), which classifies as a low-enthalpy geothermal system that utilizes the ground as a natural heat source and air as the working fluid for space cooling or heating, depending on the season. In this system, during winter, cold outdoor air is drawn through buried pipes, where it absorbs heat from the surrounding soil. As the air passes through the underground pipes, thermal energy is transferred from the soil to the outdoor air, resulting in a significant temperature increase at the outlet compared to the outdoor air. The same concept can be extended to summer [24]. If the EAHE outlet air temperature is sufficiently low, it can be supplied directly for space cooling. Otherwise, the precooled/preheated air can be further cooled/warmed using auxiliary equipment such as an Air Handling Unit (AHU). In this configuration, the EAHE contributes to overall energy savings by reducing the size of the heating/cooling coils of the AHU and definitively the load on the heat generators [25]. In the civil construction field, EAHE systems have been extensively utilized in commercial as well as residential buildings. From single-family residences to commercial structures, EAHEs have the potential to play a significant role in enhancing thermal comfort and lowering energy usage. Their applications are varied and encompass indoor heating and cooling [26], [27], [28], ventilation [29], [30], [31], process conditioning [32] and agricultural greenhouse climate control [33].

For space air conditioning, numerous studies have identified EAHEs integrated with buildings as an applicable passive energy system by benefitting from the relatively stable subsurface temperature. This underground temperature can be achieved by deploying the EAHE at a depth of 3 – 4 m. The performance of such systems primarily depends on the seasonal variation of the inlet air temperature and the pipe wall temperature, which in turn is influenced by the ground thermal conditions [34]. Based on the literature, EAHE systems are generally classified according to their pipe configuration (single, parallel, or serpentine layout), operation mode (open-loop, closed-loop, or recirculated) and installation orientation (horizontal or vertical). Horizontal systems [35] need shallower excavation and are less expensive to install; however, their thermal effectiveness is affected by fluctuations in surface temperature and soil moisture. This was demonstrated by Lattieff et al. [36], who carried out a thermal performance analysis of a horizontal heat exchanger in a subtropical climate. Vertical systems using boreholes need a reduced land area and capitalize on the more constant temperatures found in deeper soil, therefore mitigating the effects of seasonal and diurnal fluctuations. Although vertical systems provide enhanced thermal effectiveness and are favoured in urban settings, they entail higher installation expenses and need deeper digging [37]. Also the study of Huang et al. [38] examined a vertical EAHE system incorporating internally baffled pipes. This configuration requires minimal land area and provides high efficiency in the use of geothermal energy. The measured outlet air temperatures indicated strong cooling performance, with a pre-cooling capacity up to 915.9 W. An investigation conducted by Merdassi and Aouissi [39] evaluated the efficacy of two configurations of EAHE: serpentine and spiral. The findings suggest that, considering the similar thermal performance of serpentine and spiral EAHEs at the same lengths, pressure drop becomes the crucial element in determining the best design, highlighting the importance of investigating and balancing thermal effectiveness with airflow resistance. Regarding the use of EAHE in building cooling, Dehina et al. [40] introduced an innovative coaxial ground water–air heat exchanger, whereby water circulates inside an axial tube while air traverses an annular gap. The findings indicated that the system accounted for 16% of the cooling need in the analysed case study. In contrast, other studies [41], [42] investigated the efficacy of an EAHE in enhancing the interior environmental conditions in industrial buildings, finding that this system could fulfil 38% of the cooling requirements.

Overall, the findings from the previously reported studies indicate that incorporating EAHEs into building-HVAC systems yields beneficial outcomes. Nevertheless, several research studies concur that often its effectiveness alone does not adequately satisfy the cooling requirements of buildings, leading to recommendations for its hybrid use alongside other air conditioning systems.

With the ongoing advancements in technology, EAHE systems are evolving to become much more advanced and efficient. Cutting-edge design methodologies, including the application of innovative materials and smart control mechanisms, significantly improve the functionality and reliability of these systems. In this context, current investigations are centred on enhancing the synergy between EAHE and various building systems, including HVAC and ventilation systems, to improve the global energy efficiency [43]. Harrouz et al. [44] showed that the integration of an EAHE with a direct evaporative cooler (DEC) system significantly outperformed the use of a DEC alone. The hybrid configuration, indeed, resulted in reductions of more than 40% in water use and around 33.5% in power usage, respectively. Cirillo et al. [45], instead, investigated the economic and energy performance of a hybrid HVAC system functioning in both semi-closed loop and open loop configurations. The research indicates that the integration of an EAHE upstream of an HVAC system leads to substantial reductions in energy consumption, achieving reductions of up to 52% in school buildings and 71% in residential buildings during heating periods. The authors also found that the EAHE provides significant savings in cooling mode, especially during periods of elevated ventilation demand. Furthermore, they highlighted that the semi-closed loop enhances air stability and diminishes peak loads, whereas the open loop offers greater cost-effectiveness, with payback periods of 3.2 years for schools and 2.0 years for residential applications. Hybrid EAHE systems provide scalable, efficient and low-carbon solutions for HVAC applications.

Despite the extensive literature on EAHE systems and their integration within HVAC applications, several gaps remain. Most previous studies, indeed, primarily focus on outlet air temperature improvement and overall energy savings, while limited attention has been given to the impact of EAHE integration on the design capacity of the heating and cooling coils of the downstream AHU. Furthermore, comparative assessments under different European climatic conditions remain scarce, particularly for school buildings characterized by high ventilation air rates and strict indoor air quality requirements. In addition, few studies systematically investigate the influence of the EAHE pipe geometric parameters on system performance in relation to criteria of sizing HVAC system components.

Therefore, a comprehensive analysis linking EAHE geometric design, climatic context, and the reduction of design thermal capacity of the AHU coils is still lacking.

The present study addresses this gap by evaluating the contribution of an EAHE as a primary air-preconditioning stage upstream of an AHU in a school building, performing a parametric analysis of pipe dimensions and comparing results across Mediterranean and Continental climates. This approach enables a quantitative assessment of the potential reduction in AHU coil design capacity, providing practical insights for system sizing and energy-efficient HVAC design.

1.1. Innovative aspects of the research

This study introduces multiple innovative elements that aim to enhance energy performance and sustainability in school buildings by incorporating an EAHE in the HVAC system configuration. Key innovations can be summarized as follows.

- Application of an EAHE in a HVAC system for a school building**.** The use of an EAHE to improve energy efficiency in an existing school building is an innovative approach, considering that schools have specific needs like indoor thermal comfort, energy consumption and mainly indoor air quality.
- Geothermal energy integration for climate control. The utilization of geothermal energy to regulate indoor air temperature is a smart solution to reduce the energy load of HVAC systems, increasing energy efficiency without compromising comfort.
- Analyses performed in two different climatic contexts. This research provides a comparative analysis between two different climate types (Mediterranean and Continental), offering a broader understanding of the technology's potential in various climatic conditions. This approach could lead to more adaptable and scalable solutions for different regions.
- Sensitivity analysis and system optimization**.** The sensitivity analysis to optimize pipe lengths and diameters of the EAHE system allows customization of the plant based on the specific demands of buildings and their energy needs, thus enhancing efficiency and energy savings.
- Quantification of AHU design capacity requirements. This study quantifies the design thermal capacity of the AHU coils when incorporating an EAHE. This allows for an accurate assessment of the potential reduction in coil design capacity and, in the future development of research, the associated energy savings.

In summary, the innovations in this research lie in the use of geothermal technologies for climate control in school buildings, comparative analysis for different climates, system optimization through sensitivity analysis and the reduction of the HVAC system size. The overall target is to improve energy efficiency and sustainability in school buildings.

2. Methodology

The methodology focuses on assessing how an EAHE can contribute to improve the energy efficiency in school buildings considering two European climates (humid Continental and Mediterranean).

2.1. Thermal and energy modeling of the EAHE system

For this work, a 2D mathematical model of the EAHE is adopted from previous papers of the authors [43], [46]. The energy model of the EAHE adopted in the present study was previously developed, studied, and experimentally validated in those papers; in that study, the model was applied within an HVAC system framework and its reliability was thoroughly assessed.

The present study is conducted for Southern Italy and Hungary, to compare the performance of a baseline HVAC system setup (Fig. 1) with a new HVAC system configuration that includes an EAHE installed upstream of the AHU (Fig. 2).

To guarantee significant energy savings, the air is pre-treated by an EAHE placed upstream of the AHU, in order to quantify the reduction of the design capacity of the heating and cooling coils of the AHU. The EAHE plays a role in pre-conditioning the outdoor air by cooling or heating it before it arrives to the AHU.

The hybrid HVAC system operates in an open-loop configuration. The AHU provides the renewal of the indoor air by maintaining good air quality inside the building. The EAHE system has 40 horizontally embedded pipes in parallel at a ground depth of 2.5 m. It should be noted that the analysed system is a horizontal earth-to-air heat exchanger and not a deep geothermal borehole. At this depth (2.5 m), the soil temperature is primarily governed by seasonal thermal variations [47]. Due to the relatively low heat exchangers and the natural seasonal regeneration of the surrounding ground [48], long-term soil thermal drift effects are expected to be negligible. Therefore, the assumption of steady-state soil conditions can be considered acceptable for the time scale investigated in this study.

In the numerical model, the EAHE system was simplified as a single equivalent horizontal pipe to reduce computational complexity. However, in the proposed installation, the distance between two adjacent pipes is 2.5 m. According to the literature [47,48], such spacing is sufficient to ensure that thermal interference between adjacent horizontal heat exchangers remains negligible under typical operating conditions. Therefore, the assumption of negligible thermal interaction among adjacent pipes is considered reasonable and does not significantly affect the simulation results.

The EAHE pipes are installed with a slight longitudinal slope to ensure gravity-assisted drainage of condensate, thereby preventing water stagnation and mitigating potential long-term effects on thermal performance and pipe durability. Indeed, during summer operation, when humid outdoor air is cooled below its dew-point temperature inside the EAHE, condensate can form on the inside surface of the pipe. To avoid water stagnation and hygiene/performance problems, a standard installation strategy is to lay the buried pipes with a small continuous longitudinal slope (on the order of ~1–2%) toward a condensate collection chamber located at the lowest point, accessible for inspection and cleaning. The collected condensate is discharged into a safe drainage (building drainage or dedicated collection tank), preferably through an airtight sealed branch to prevent air leakage and odour ingress into the ventilation airflow. Fig. 3 reports the scheme of the system.

In the research, multiple pipes lengths (20, 40, 60, 80 and 100 m) and diameters (0.5 m, 0.3 m and 0.2 m) are analysed. Air flow rate is kept constant to ensure the achievement of the design air change rate of the school building, causing air velocity to change accordingly inside EAHE pipes ($v = 0.38$ m/s, $v = 1.04$ m/s and $v = 2.38$ m/s). For the considered operating conditions, the Reynolds number is approximately 2.83×10^4 ($D = 0.2$ m), 1.84×10^4 ($D = 0.3$ m), and 1.14×10^4 ($D = 0.5$ m). Since all values are well above the critical threshold for turbulent flow ($Re \approx 4000$), the airflow inside the pipe is fully turbulent, ensuring adequate convective heat exchange, further supported by the air residence time within the duct. This is true also for the minimum air velocity (0.38 m/s, in the case of $D = 0.5$ m).

Based on the previous research, the EAHE model focuses exclusively on a single pipe, with the surrounding soil extending to a depth

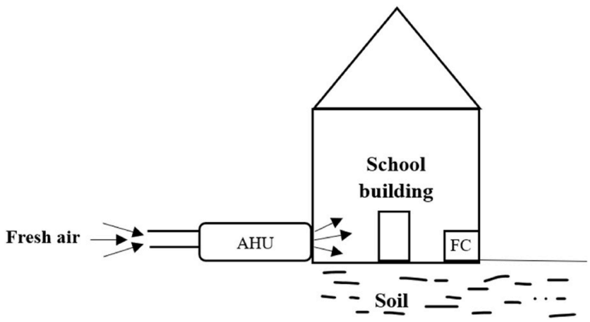

Fig. 1. Baseline configuration of the existing HVAC system (AHU + fan-coils FCs).

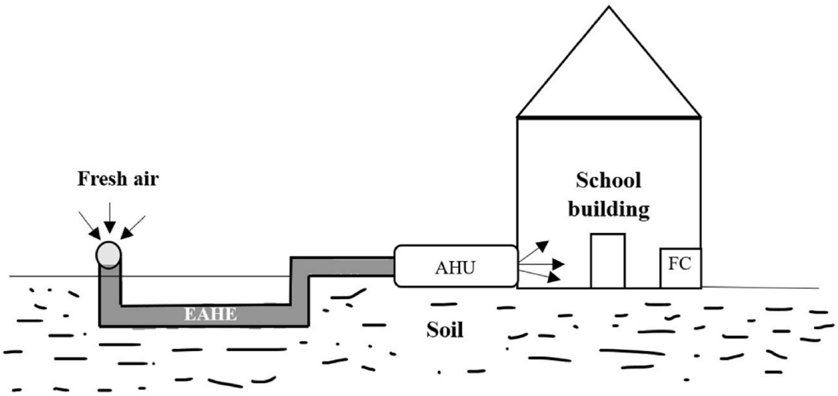

Fig. 2. The proposed new configuration of a hybrid EAHE-AHU system and fan coils (FCs).

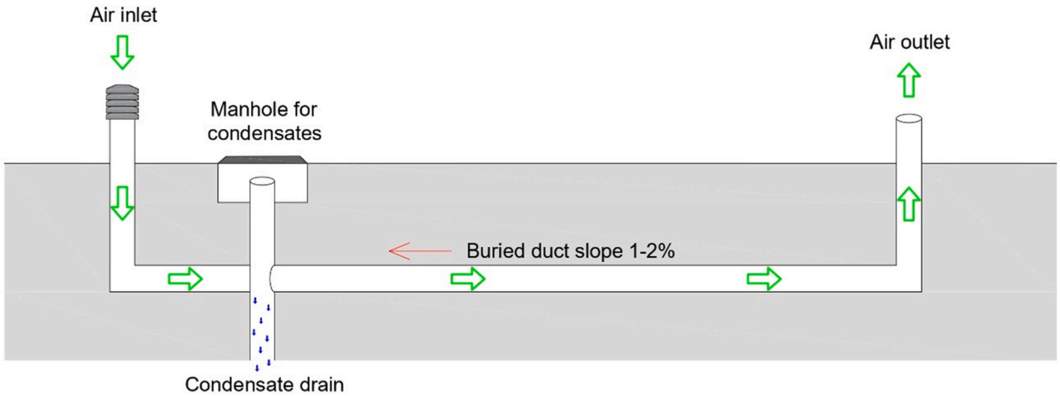

Fig. 3. Scheme of the EAHE drainage system.

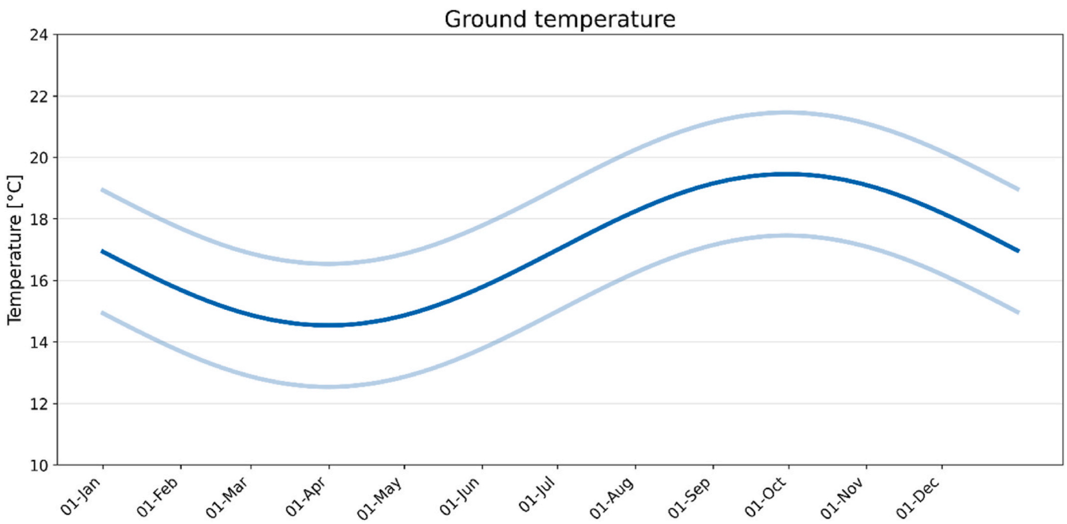

Fig. 4. Ground temperature in Naples at the EAHE burial depth of 2.5 m, obtained applying the Kusuda–Achenbach equation (calculated value and uncertainty band).

of 20 m. The temperature of the ground is determined using the Kusuda–Achenbach equation [49]:

$$T_g(x,t)\ [^\circ C] = T_m - A \exp\left(-x \cdot \sqrt{\frac{\pi}{P\alpha_g}}\right)\cos\left[\frac{2\pi}{365}\left(t - t_{Tmin} - \frac{x}{2}\sqrt{\frac{P}{\pi\alpha_g}}\right)\right] \tag{1}$$

where:

$T_g(x,t)$: ground temperature at depth x [m] and time t [s]; A: soil surface temperature fluctuation amplitude [°C]; T_m: average soil surface temperature [°C]; α_g: thermal diffusivity [m^2/day]; P: analysis period (365 days); t_{Tmin}: state constant of the soil surface [days].

Using Eq. (1), the soil temperature at the EAHE burial depth $x = 2.5$ m is season-dependent but exhibits an attenuated, phase-shifted annual oscillation around the mean soil surface temperature. For Naples, the Kusuda–Achenbach model yields an annual mean ground temperature of 17.0 °C at the considered depth, with an annual variation of approximately 14.5–19.5 °C (Fig. 4). For the winter and summer design conditions adopted for the AHU coil sizing, the predicted ground temperature at 2.5 m remains close to the mean value (~16.9 °C in early January and ~17.2 °C in early July). Accordingly, in the present design-day sizing analysis a representative value of 17.0 °C is adopted for Naples. Similarly, for Budapest the Kusuda–Achenbach model yields an annual mean ground temperature of 12.3 °C at $x = 2.5$ m, with an annual variation of approximately 9.8–14.8 °C (Fig. 5). For the winter and summer design conditions adopted in this study, the predicted ground temperature at 2.5 m remains close to the mean value (~12.1 °C in early January and ~12.4 °C in early July). Therefore, a representative value of 12.3 °C is adopted for Budapest in the present design-day sizing analysis.

The thermal profile of the ground is a crucial aspect in the EAHE's design. The locality's climate conditions where the EAHE system is employed influence the thermal performance of the system. Hence, the school building simulation is performed considering both climates of Naples and Budapest for comparison.

The results are derived under steady design thermal-hygrometric conditions representative of summer and winter peaks to quantify the AHU coil design capacities and their reduction due to the EAHE. Accordingly, the outdoor air state is assumed constant at the selected design condition for each mode (summer/winter), which is consistent with standard practice for coil sizing at peak conditions. The outdoor air design dry bulb temperatures and mean coincident wet bulb (MCWB) temperatures for Naples and Budapest are taken from ASHRAE design conditions, according to 99% occurrence based on ASHRAE handbook [50]. The corresponding outdoor relative humidity is calculated from the paired dry bulb and wet bulb temperatures through standard psychrometric relations. All remaining moist air properties (humidity ratio and specific enthalpy) are computed consistently from this basis (see Tables 1 and 2).

The EAHE outlet temperature is used as an input to AHU before air is supplied to the school building. In this section the methodology used for the following analyses is reported:

- calculation of the outlet air temperature of the EAHE system using several pipe geometries;
- calculation of the contribution of the EAHE to the sizing reduction of the AHU coils for summer and winter in Mediterranean climate;
- calculation of the contribution of the EAHE to the sizing reduction of the AHU coils for summer and winter in Continental climate;
- calculation of the attained Coefficient of Performance (COP) for the hybrid EAHE – AHU system.

The total outdoor air flow is calculated based on school building design occupancy and area according to the Standard EN 16798-1

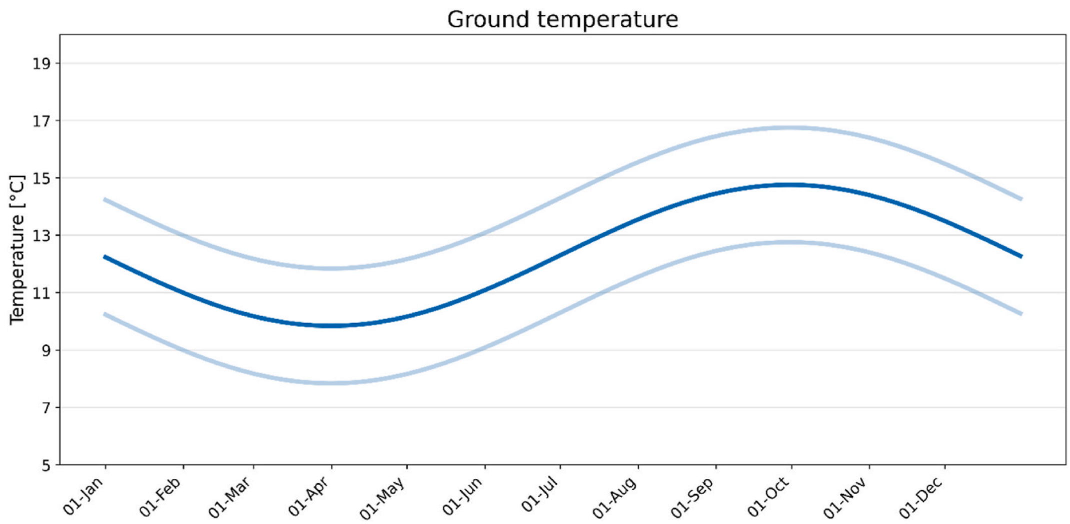

Fig. 5. Ground temperature in Budapest at the EAHE burial depth of 2.5 m, obtained applying the Kusuda–Achenbach equation (calculated value and uncertainty band).

Table 1
Humid air properties in the basic HVAC system at summer design conditions.

	Naples				Budapest			
	T	Φ	ω	h	T	Φ	ω	h
	[°C]	[%]	[g/kg]	[kJ/kg]	[°C]	[%]	[g/kg]	[kJ/kg]
Design outdoor air conditions	31.8	50	14.8	69.96	32	46.7	14	68.01
Air conditions after the cooling coil in the AHU	11.9	100	8.7	33.91	11.9	100	8.7	33.91
Supply air conditions	13	92.95	8.7	35.03	13	92.95	8.7	35.03

Table 2
Humid air properties in the basic HVAC system at winter design conditions.

	Naples				Budapest			
	T	Φ	ω	h	T	Φ	ω	h
	[°C]	[%]	[g/kg]	[kJ/kg]	[°C]	[%]	[g/kg]	[kJ/kg]
Design outdoor air conditions	2.3	55	2.45	8.46	−9.1	65	1.23	−6.11
Air conditions after the heating coil in the AHU	20	16.96	2.45	26.32	20	8.53	1.23	23.23
Supply air conditions	20	43.42	6.38	36.31	20	43.42	6.38	36.31

[51]. The design ventilation air rates for the dilution of indoor air contaminants and ventilation rates per individual are defined according to two different criteria: per unit floor area and per occupant, respectively. The first one is set at 0.35 l/s per square meter of floor area, with no specific requirement per person, while the second one is set at 7 l/s per person, without a corresponding value defined per unit area. These two rates of ventilation are calculated and then added together; a total airflow rate of 10692 m^3/h is finally obtained.

Indoor air temperature setpoints are 20 °C in winter and 26 °C in summer, both at 50% relative humidity (ϕ). To guarantee optimal thermal comfort for the building's occupants throughout working hours and the internal thermo-hygrometric design conditions, a setpoint temperature of the supply air equal to 13 °C in summer and 20 °C in winter is chosen. The supply air temperature of 13 °C refers to the primary air delivered by the AHU in summer conditions and is selected to obtain the sufficient dehumidification of the supply air while minimizing the re-heating coil thermal capacity; in the considered air-water mixed system, the AHU covers only the latent load and the ventilation requirements, while the sensible space load is handled by the hydronic terminal units (fan-coils).

Based on the mass balance equation (Eq. (2) and (3)) for the air-conditioned rooms, the humidity ratio values ω_s of the supply air are estimated as 8.7 g/kg in summer and 6.38 g/kg in winter. Then, by using the psychrometric chart, the relative humidity ϕ values are evaluated as 92.95% and 43.42% for summer and winter, respectively.

$$\dot{m}_a\omega_s + \dot{m}_v = \dot{m}_a\omega_r \tag{2}$$

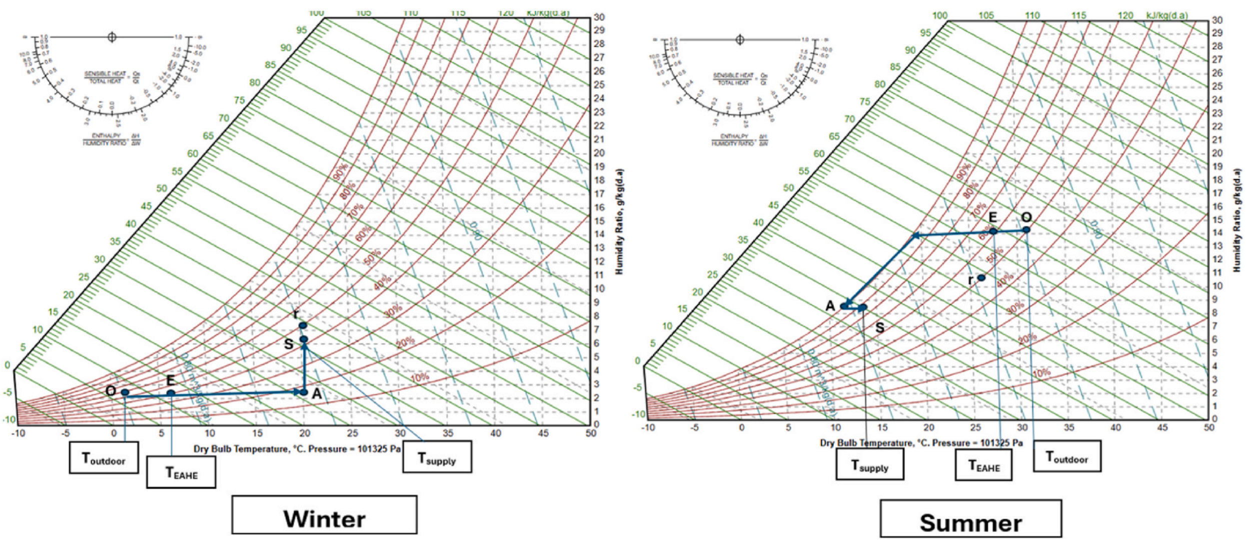

Fig. 6. Representation, on the psychrometric chart, of the humid air treatment processes in the AHU for heating and cooling modes in Naples, with and without the EAHE.

$$\omega_s = \omega_r - \frac{\dot{m}_v}{\dot{m}_a} \tag{3}$$

where: $\dot{m}_a$ is the air mass flow rate, $\dot{m}_v$ is the occupant's total mass flow rate of vapor; ω_r is the humidity ratio value of the air to be obtained in the rooms.

Tables 1 and 2 report the properties of the air in the following conditions (for the basic HVAC system): design outdoor air conditions; air conditions after the cooling or heating coil in the AHU; supply air conditions.

In the typical air-water HVAC configuration, the active components of the AHU are: filters; blower (supply fan); in winter, hydronic heating coil and vapor humidifier; in summer, cooling and dehumidification coil plus re-heating coil. Figs. 6 and 7 depict, on the psychrometric chart, the humid air processes in the EAHE and in the AHU for the proposed innovative system, as follows:

- in summer: cooling and dehumidification plus re-heating are used to reach the required setpoint for the supply primary air ($T_{ba} = 13\ ^\circ C$; $\omega = 8.7$ g kg^{-1});
- in winter: heating plus vapor humidification is used to reach the required setpoint for the supply primary air ($T_{ba} = 20\ ^\circ C$; $\omega = 6.38$ g kg^{-1}).

In the chart, point 'O' refers to the design outdoor air conditions, point 'E' to the air conditions at the EAHE outlet, point 'S' to the supply air conditions and 'r' to the design indoor conditions to guarantee thermal comfort. Therefore, $T_{outdoor}$ is the temperature of external air, T_{EAHE} refers to the air conditions at the EAHE outlet and T_{supply} is the temperature of supply primary air. Point 'A' represents the air conditions downstream of the heating/cooling coil: in winter conditions, it corresponds to the humid air leaving the heating coil before steam humidification, whereas in summer conditions it represents the air state after the cooling and dehumidification process before re-heating.

To assess the capacity of the coils, mass and energy balance calculations are performed on a specific control volume. The cooling coil and the re-heating coil are active in summer. equation (4) is the energy balance used to calculate the design cooling capacity (in the basic configuration without EAHE):

$$\dot{Q}_{cc} = \dot{m}_a (h_o - h_A) - \dot{m}_{a,co} h_{co} \tag{4}$$

where Q_{cc} is the design capacity of the cooling coil in kW, m_a is the air mass flow of the air in kg/s, h_o and h_A are the specific enthalpy in kJ/kg of the outdoor air and of the air after the cooling and dehumidification process, respectively; $m_{a,co}$ is the condensed water mass flow in kg/s, and h_{co} is the specific enthalpy of the condensed water in kJ/kg. The (Eq. (5)) is used to calculate the re-heating coil capacity:

$$\dot{Q}_{ReH} = \dot{m}_a (h_s - h_A) \tag{5}$$

where Q_{ReH} is the capacity of re-heating process in kW, h_s and h_A are the specific enthalpy in kJ/kg of the supply air and of the air after the cooling and dehumidification process, respectively.

Heating coil and vapor humidifier are active in winter. The design heating capacity is calculate based on the following energy

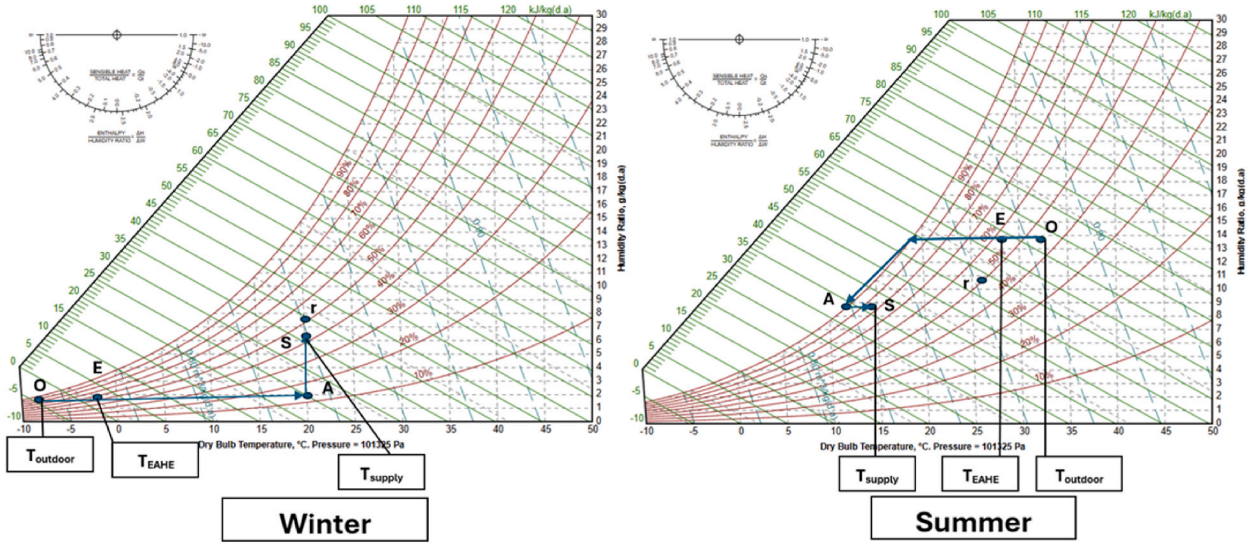

Fig. 7. Representation, on the psychrometric chart, of the humid air treatment processes in the AHU for heating and cooling modes in Budapest, with and without EAHE.

balance, equation (6) (in the basic configuration without EAHE):

$$\dot{Q}_{He} = \dot{m}_a (h_A - h_o) \tag{6}$$

where Q_{He} is the design capacity of the heating coil in kW, h_o and h_A are the enthalpy in kJ/kg of the outdoor air and of the air after the heating process, respectively.

When considering the EAHE, the capacity of the AHU coils both in summer and winter is reduced as below reported, because the air entering the AHU is in condition E (air at the EAHE outlet) instead of O (outside air).

Equation (7) computes the heat transfer capacity of the processed air stream within EAHE by considering the inlet and outlet temperatures:

$$Q_{EAHE} = \dot{m}_a \left| (h_{a,in} - h_{a,out}) \right| \tag{7}$$

where Q_{EAHE} is the preheating or precooling capacity of the EAHE system in kW, in winter and summer, respectively; $h_{a,in}$ is the specific enthalpy of air entering the EAHE system in kJ/kg and $h_{a,out}$ is the specific enthalpy of air at the outlet of EAHE in kJ/kg.

The mass of condensed water in the EAHE in summer is derived by a moisture mass balance expressed as (Eq. (8)):

$$\dot{m}_{cond} = \dot{m}_a \, (\omega_O - \omega_E) \tag{8}$$

The dry air mass flow rate is denoted as $\dot{m}_a$, whereas ω_O and ω_E are the specific humidity of the air at the inlet (outside air) and the exit of the EAHE, respectively.

The fan power (W_{fan}) can be determined by (Eq. (9)) as:

$$W_{fan} = \frac{\dot{V} * \Delta p}{\eta_{fan}} \tag{9}$$

where $\dot{V}$ is the air total volumetric flow rate in m^3/s; Δp is the pressure drop of the EAHE + AHU system in Pa and η_{fan} is the efficiency of the blower (fan).

A standard parameter of the EAHE to quantify how close the temperature of the air exiting the EAHE is to the ground temperature is the heat exchanger effectiveness (ε). For both heating and cooling modes, the effectiveness is defined as the ratio between the temperature change of the air achieved and the maximum possible change relative to the ground temperature (Eq. (10)):

$$\varepsilon = \frac{|T_{in} - T_{EAHE,out}|}{|T_{in} - T_g|} \tag{10}$$

where:

T_{in}: inlet air temperature (°C), which is the outdoor temperature.

$T_{EAHE,out}$: outlet air temperature (°C) at the end of the EAHE system.

T_g: ground temperature (°C) at the pipe depth.

Effectiveness is a purely thermal indicator ($0 \le \varepsilon \le 1$) and does not account for pressure losses or fan electricity.

To evaluate the overall energy performance of the EAHE system (including the fan electric power), the Coefficient of Performance (COP) is defined as the ratio of useful thermal power exchanged in the EAHE to the fan electric power:

$$COP_{EAHE} = \frac{|\dot{Q}_{EAHE}|}{\dot{W}_{fan}} \tag{11}$$

where $|\dot{Q}_{EAHE}|$ is the magnitude of the heating rate provided by the EAHE (computed from Eq. (7)) and $\dot{W}_{fan}$ is the fan electric power (Eq. (9)). With this sign convention, COP_{EAHE} is always positive and can be directly compared between seasons: in winter it represents the heating benefit (air pre-heating), while in summer it represents the cooling benefit (air pre-cooling). Therefore, two EAHE geometries may exhibit similar effectiveness ε (similar thermal approach to T_g) but different COP_{EAHE} due to different pressure losses and fan electric power.

2.2. Investment and maintenance costs of the EAHE system and avoided investment costs associated with the reduced heating/cooling design capacities of the AHU coils

To complement the design sizing analysis, an investment cost assessment is performed for all EAHE geometries investigated (pipe lengths 20–100 m and diameters 0.5/0.3/0.2 m). The EAHE field consists of $N_p = 40$ horizontal parallel pipes. The total initial investment is computed by separating pipe procurement, earthworks (excavation and refilling/compaction), and auxiliary elements (collectors/joints and drainage/inspection). For a given diameter D and pipe length L, the total installed pipe length is:

$$L_{tot} = N_p \, L \tag{12}$$

The EAHE investment cost is then evaluated as:

$$C_{\mathrm{EAHE}}(D,L) = L_{\mathrm{tot}}\, c_{\mathrm{pipe}}(D) + V(D,L)\,\left(c_{\mathrm{exc}} + c_{\mathrm{ref}}\right) + \alpha_{\mathrm{fit}}\, L_{\mathrm{tot}}\, c_{\mathrm{pipe}}(D) + C_{\mathrm{drain}} \tag{13}$$

where $c_{\mathrm{pipe}}(D)$ is the unit pipe cost, c_{exc} and c_{ref} are the unit costs for excavation and refilling/compaction, respectively, and α_{fit} accounts for collectors, joints and fittings as a fraction of the pipe procurement cost. The excavation volume is approximated as:

$$V(D,L) = w(D)\; h\, L_{\mathrm{tot}} \tag{14}$$

with $h = 2.5$ m and $w(D)$ the assumed trench width (taken as the commercial outer diameter associated with the selected nominal size plus a fixed lateral allowance). The term C_{drain} groups together drainage and inspection elements required for safe operation and maintenance access (treated as a lump-sum cost at field level).

Because the EAHE reduces the design heating and cooling coil capacities of the AHU, an avoided coil investment cost is computed as a reduction. The baseline coil costs $C_{\mathrm{H,base}}$ and $C_{\mathrm{C,base}}$ are defined at the design airflow rate of the case study, and the reduced costs are estimated assuming a first-order proportionality to the design capacity at a fixed airflow:

$$C_{\mathrm{coil,new}} \approx C_{\mathrm{coil,base}} \left(\frac{Q_{\mathrm{new}}}{Q_{\mathrm{base}}}\right) \tag{15}$$

This scaling is applied separately for the heating and cooling coils using the coil design capacities Q_{new} obtained for each EAHE geometry; the avoided coil investment cost is then given by $C_{\mathrm{coil,base}} - C_{\mathrm{coil,new}}$.

Pipe supply costs are taken from commercial prices considering the adopted diameters, while excavation, refilling and compaction costs are derived from public works price lists. The excavation volume is estimated from the burial depth, the total installed pipe length, and an assumed trench width equal to the pipe outer diameter plus a fixed lateral allowance. Detailed executive design of manifolds, junctions and condensate drainage are outside the scope of the present study. For this reason, these aliquots are calculated considering 10% of pipe cost for collectors and joints and a fixed cost of 2000 EUR plus 3% of pipe cost for drainage and inspection equipment.

Furthermore, annual maintenance expenses are calculated as follows:

$$C_{\mathrm{maint,ann}} = C_{\mathrm{fix}} + C_L\, L_{\mathrm{tot}} \tag{16}$$

where C_{fix} accounts for routine actions that are primarily driven by IAQ and operability assurance (filter replacement and cleanout of the intake and condensate collection point) and C_L represents deep cleanout costs to be performed once in 10 years that vary with the pipe length L_{tot}.

Fixed yearly maintenance expenses are quantified in 150 €/year, while the costs of deep cleanout and disinfection of pipes are considered equal to 6 EUR/m, 8 EUR/m, and 12 EUR/m as a function of the pipe diameter. These last costs are considered every 10 years as the EAHE presents a condensate drainage system.

3. Case study

The case study is a school building located in Naples (Southern Italy, Lat. 40° 50′ 49.20″ N; Long. 14° 15′ 54.00″ E). The building serves as a kindergarten for kids aged 3 to 5. The entire floor space of the educational facility is about 1534 m^2, with an interior height of 3.3 m, comprising two floors above ground. It fits 347 people and has 7 classrooms along with other rooms. Table 3 reports details regarding space, volume and occupancy for each room. The present analysis focuses on peak design conditions for sizing of the AHU heating and cooling coils; therefore, the results are independent of specific occupancy schedules or intermittent operational periods typical of school buildings. Fig. 8 offers a 3D representation of the case study building, while Fig. 9 displays the architectural plans,

Table 3
Occupancy level, area and volume for each room forthe case study building.

Chamber	Occupant's Number	Area (m^2)	Volume (m^3)
Class 1	36	143.3	472.9
Class 2	34	137.4	453.3
Class 3	34	137.4	453.3
Class 4	34	137.4	453.3
Class 5	34	137.4	453.3
Class 6	34	136.7	451.1
Class 7	35	140.7	464.2
Kitchen	2	17.4	57.5
Canteen	53	109.9	362.6
Relaxing area	8	37.1	122.4
Boardroom	6	24.6	81.2
Office 1	4	36.6	120.9
Office 2	2	20.9	68.8
Office 3	2	22.6	74.7
Medical room	2	13.68	44.8
Hallway	25	271.4	895.5

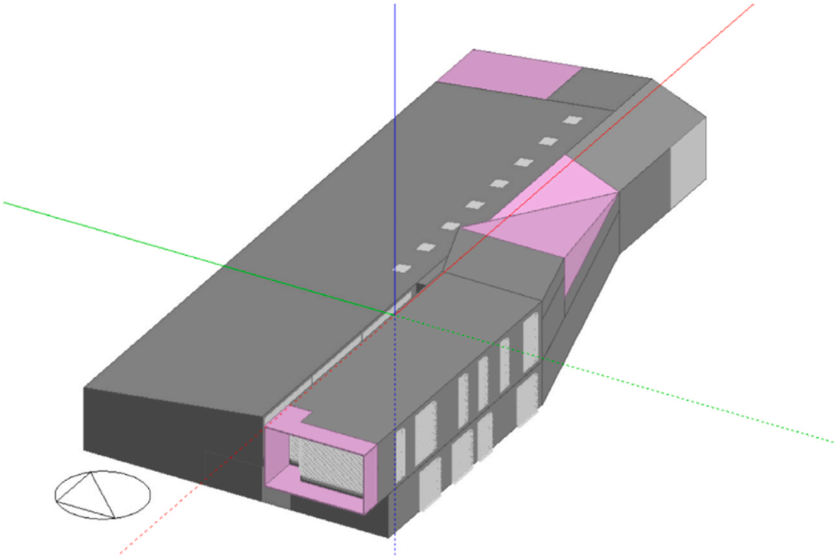

Fig. 8. 3D representation of the geometry of the school building used in the case study.

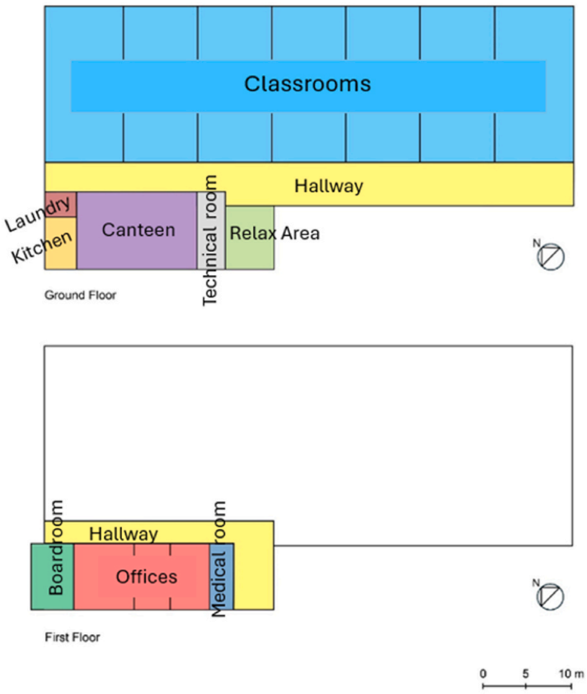

Fig. 9. Building plans for the ground and first floors.

Table 4
Thermal transmittance of the building envelope components.

Building envelope component	Thermal transmittance (U) [W/m^{2}K]
Windows	1.70
Floor	0.27
Wall	0.19
Roof	0.26

depicting the intended use of each space.

The building envelope has been designed in compliance with current Italian energy efficiency rules for buildings. Table 4 displays the thermal transmittance for opaque and glazed components of the building envelope.

3.1. Climate classification

Based on the Köppen classification, Naples is classified as Csa (hot-summer Mediterranean climate), while according to DPR 412/93 [52] Naples has 1034 Heating Degree Days (HDD) and is classified as belonging to winter climatic zone C. The climate classification of Budapest according to the Köppen system is Dfb, which indicates a humid temperate climate associated with very warm summers and chilly winters. Specifically, in the Köppen classification the 'C' stands for a temperate climate, the 'f' indicates precipitation recorded within a year (without a unique dry season), whereas the 'a' indicates very warm summers, with mean temperature of the hottest month exceeding 22 °C. Budapest city has 3105 HDD according to ASHRAE [50]. The outdoor air design temperature in summer $T_{summer\ design}$ for Budapest is between 33 °C and 31.1 °C based on ASHRAE, so in this study 32 °C is selected, and $T_{summer\ design}$ for Naples is equal to 31.8 °C. The outdoor $T_{winter\ design}$ is −9.1 °C and 2.3 °C for Budapest and Naples respectively.

3.2. Description of the HVAC system

The HVAC system consists mainly of an Air Handling Unit and circular air ducts for primary air, hydronic fan-coils for heating and cooling and heat pumps as heating and cooling generators. These are two reversible ("invertible") electric air-to-water heat pumps, together rated at 120 kW nominal power for heating and 160 kW nominal power for cooling with Coefficient of Performance (COP) of 3.8 and Energy Efficiency Ratio (EER) of 4.2. The water distribution is provided by insulated copper ducts located inside the building's structure. The heating system operating period for Budapest is equal to 10 h daily, from 15th of September to 15th of May (according to Hungarian regulations [53]), while the cooling system operates for 4 h daily, from mid-June to July. For Naples the operational periods are from 15th of November to 31st of March for 10 h per day (according to Italian regulations [52]) and from June to July for 6 h per day, for heating and cooling, respectively. The AHU operates continuously during occupancy hours. The domestic hot water (DHW) is produced using a suitable electric air-to-water heat pump. Table 5 delineates the main attributes of the primary air, cooling/heating and DHW systems.

According to Hungarian regulations, the operating period for a heating system is established from 15 September until the end of March.

4. Results and discussion

This study evaluates the thermal performances of an HVAC system characterized by an EAHE linked to an AHU. The thermal operation of the EAHE is influenced by the EAHE geometry, soil temperature and climatic settings. The soil temperature closely aligns with the outdoor air average yearly temperature of the location where the EAHE is installed; as a result, it tends to be higher than the real outdoor temperature during winter and lower during summer. This study focuses on an EAHE which features a horizontal configuration, with soil temperatures recorded at 12.3 °C and 17 °C for Budapest and Naples, respectively. As aforementioned, the aim of this research is to find the reduction in the design thermal capacity of the heating and cooling coils of the AHU obtained from the EAHE – AHU hybrid HVAC system for a school building in two different climatic conditions.

4.1. Thermal and energy analysis of the EAHE – AHU hybrid HVAC system

Figs. 10 and 11 illustrate the ground temperature at 2.5 depth and the air temperature at the exit of the EAHE for different lengths of the EAHE pipes during summer and winter, considering different tube diameters, for the two analysed locations. The increase in air speed occurs as the duct diameter decreases, which provides an enhancement in the heat transfer coefficient for convection, ultimately

Table 5
Main characteristics of primary air, cooling/heating and domestic hot water systems.

System	Characteristic	Value
Primary air	Supply outdoor air flow rate	10692 [m^3/h]
	Air Handling Unit with hydronic coils	
	Fan power	Min 2.1 Max 2.2 [kW]
Cooling/Heating	System type: hydronic fan-coils plus air-to-water heat pumps	
	Total cooling/heating capacity	160/120 [kW]
	Efficiency of the distribution	0.9
	COP/EER of the air-water heat pump	3.8/4.2
	Efficiency of the emission	0.9
Domestic Hot Water	System type:	
	300 L tank and electrical air-to-water heat pump	
	Thermal power	12 [kW]
	Efficiency of the distribution	0.9
	COP of the dedicated air-water heat pump	3.5

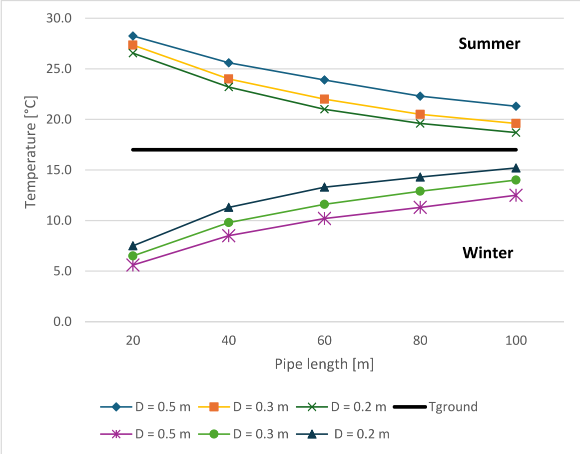

Fig. 10. Air temperature at the EAHE exit for different pipe diameters and lengths, Naples.

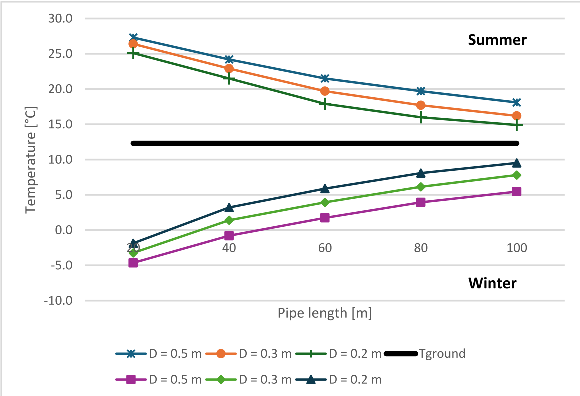

Fig. 11. Air temperature at the EAHE exit for different pipe diameters and lengths, Budapest.

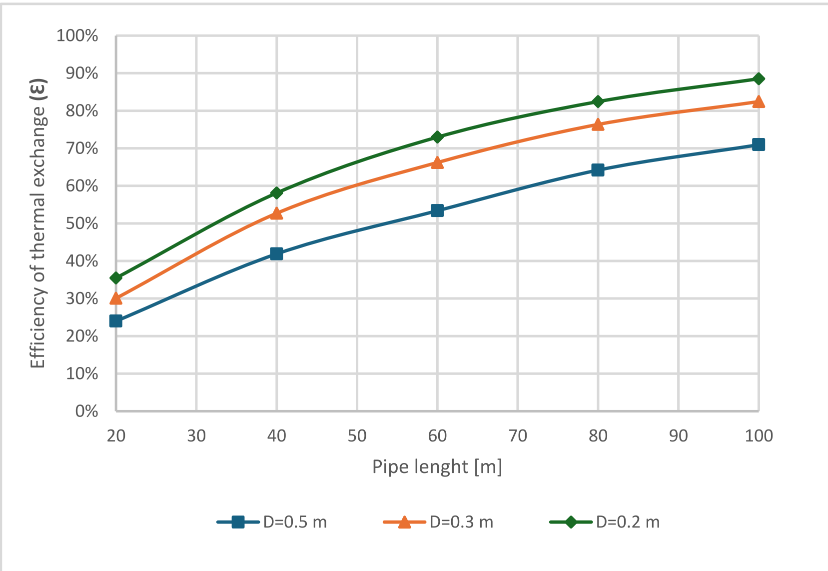

Fig. 12. EAHE thermal effectiveness as a function of pipe length and diameter for Naples and Budapest in summer season.

leading to improved heat exchange. As it can be seen in Figs. 10 and 11, utilizing the smallest inner tube diameter (D = 0.2 m, associated with an inlet air velocity of 2.38 m/s) allows for a more significant air temperature variation in the EAHE.

The thermal effectiveness of the EAHE as a function of the pipe diameter and length for the two cities is presented in Figs. 12 and 13. For the two locations, the results indicate that the thermal effectiveness during winter and summer is comparable, which explains the use of a single graph applicable to both the cities. The highest ε (0.88) was obtained at length of 100 m with a diameter of 0.2 m and it indicates that an EAHE with these dimensions very effectively pre-heats/cools the outdoor air before it enters AHU.

In the two selected locations, the integration of the EAHE leads to a significant reduction in the heating and cooling design thermal capacity of the coils within the AHU, in both winter and summer, as below reported (Figs. 14–17).

During the summer operation, the incoming air exhibited elevated values of temperature and moisture content. As the air flows and passes through the EAHE, sensible heat is transferred to the surrounding soil, resulting in a thermal transformation that corresponds to a gradual decrease in air temperature. Furthermore, as the incoming air cools and saturation conditions are achieved, a hygrometric transformation (air dehumidification and water vapor condensation) may occur. For both climates, the design cooling capacity trend presents notable deviations at specific lengths of EAHE pipes due to the attainment of water vapor condensation within the EAHE. In Naples, for a diameter of 0.5 m, the cooling capacity curve diverges from the expected monotonic trend when the pipe length increases from 80 m to 100 m. Similarly, this behaviour is observed in Budapest across various configurations: for 0.2 m pipe diameter from 50 to 100 m, for 0.3 m pipe diameter between 60 and 100 m and for 0.5 m pipe diameter at length of 100 m. The sudden shift in performance for all these cases corresponds to the air inside the buried pipe reaching its dew-point temperature, resulting in moisture condensation on the inner duct surface. However, the mass flow rate of condensed water (determined using Eq. (8)) is assessed as a relatively small quantity, reaching a highest of 0.0045 kg/s in Naples and 0.0122 kg/s in Budapest for the configuration L = 100 m and D = 0.2 m. These values suggest that condensation impacts the shapes of performance curves; however, its quantitative effect on the reduction of the AHU coil thermal capacity is relatively minor when compared to the impact of the sensible heat exchange in the EAHE.

With reference to winter conditions, in December to guarantee the school building thermal comfort by raising the outdoor air temperature from −9.1 °C, 65 % RH in Budapest and from 2.3 °C, 55 % RH in Naples to the desire supply set-point 20 °C, $\omega = 6.38$ g kg^{-1}, the baseline heating coil must provide 65.1 kW in Naples and 106.8 kW in Budapest. Upon integrating the EAHE into the existing configuration, the resulting reduced values are documented in Tables 6–11. The letters E, A and S denote the air conditions after the EAHE, the air conditions after the heating coil, and the supply air conditions (post-humidification), respectively. Case (a) is for Naples and (b) for Budapest.

The proposed hybrid HVAC (EAHE + AHU) system confirmed its potential as an effective heating passive technique by demonstrating a great reduction in the design capacity of the heating coil. The finding illustrated that both the diameter and length of the pipe deeply impact the results. The design heating coil capacity decreased by 18.6% and by 15.3% with an EAHE diameter of 0.5 m and length of 20 m, reaching a 57.6% and 50% with 100 m pipe length for Naples and Budapest respectively (Figs. 18 and 19). This clearly indicates the gradual improvement in thermal exchange as the length of the pipe increases, allowing the air to remain in contact with the surrounding soil for a more extended duration. In fact, the most substantial enhancement in performance was observed with a pipe measuring 0.2 m in diameter and extending 100 m in length, where the design capacity required by the AHU heating coil was reduced to 38.5 kW in the case of Continental climate and to 17.7 kW in the case of Mediterranean climate. This result corresponds to a significant capacity reduction compared to the baseline case without EAHE, equal to 64% for Budapest and 72.9 % for Naples.

With reference to summer conditions, for the current baseline configuration, the design capacity of the AHU cooling coil is 130.8 kW and 123.8 kW in Naples and in Budapest, respectively, to reach 13 °C and $\omega = 8.7$ g kg^{-1}, which is the supply set point of the primary air. The results about the reduction of such capacity by integrating EAHE upstream of the AHU are presented in Tables 12–17. The properties of humid air after the EAHE are represented by letter E, post cooling coil air conditions by A and the supply air (after post-heating) by S.

A smaller reduction of cooling coil capacity is observed using EAHE with diameter of 0.5 m (v = 0.38 m/s) and pipe length of 20 m for both cites (10.2% in Naples and 14.3% in Budapest, Figs. 20 and 21). A reduced pipe diameter enhances convective heat transfer within the pipe. Therefore, by extending the pipe length to 100 m and using smaller diameter equal to 0.2 m (v = 2.38 m/s), the outcomes show the lowest design cooling capacity (70.1 kW in Naples and 28.7 kW in Budapest). This corresponds to a significant reduction in the coil capacity compared to the baseline scenario without EAHE (76.8% for Budapest and 46.4% for Naples).

It is very important to highlight that all these relevant reductions in thermal capacity of the AHU heating and cooling coils lead to significant reductions in thermal power of the heat generators (heat pumps), although these results are not reported in this study.

Figs. 22–25 show the winter and summer COP of the hybrid EAHE–AHU system for different pipe diameters and lengths in Naples and Budapest. In both locations, COP increases with pipe length and with decreasing pipe diameter, as the longer pipes and smaller diameters enhance the heat exchange with the ground and increase air residence time in the EAHE; the gain, however, tends to stabilize beyond about 80 m, indicating diminishing returns for additional excavation. Overall, the system performs better in the Continental climate of Budapest than in Naples, because the higher temperature difference between outdoor air and deep soil increases the useful heat that can be extracted or rejected through the EAHE. The highest COP values (30.5 and 42.4 for winter and summer, respectively) are obtained in Budapest for a pipe length of 100 m and diameter of 0.2 m, confirming that the fan power demand remains small compared with the useful thermal energy delivered.

Fig. 26 shows the variation of the fan power when using different pipe diameters and lengths. It can be noted that with a diameter of 0.2 m, although this smaller diameter improves heat transfer, it simultaneously increases frictional losses and the associated fan power. Thus, optimal EAHE design cannot be determined solely by thermal effectiveness but should be based on a multi-objective optimization approach that balances heat exchange performance with ventilation energy requirements.

From a system-level perspective, the coil capacity reductions obtained in this study are consistent with, and in some cases larger

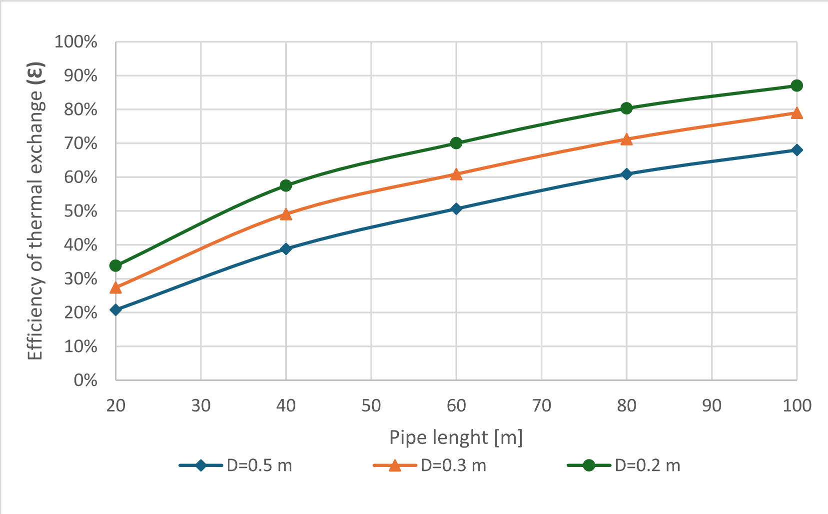

Fig. 13. EAHE thermal effectiveness as a function of pipe length and diameter for Naples and Budapest in winter season.

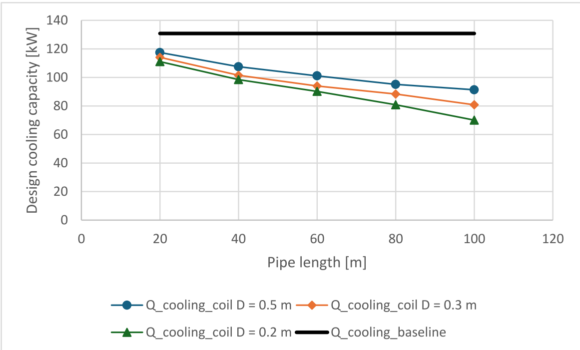

Fig. 14. Variation of the design cooling coil thermal capacity with EAHE in Naples.

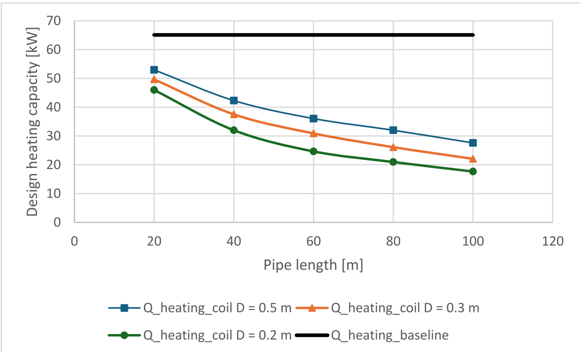

Fig. 15. Variation of the design heating coil thermal capacity with EAHE in Naples.

than, those reported in previous EAHE–HVAC integration works. D'Agostino et al. investigated a similar EAHE pre-treating unit coupled to an air-conditioning system in several worldwide climates and found that, for a duct length of 100 m, the coil capacity reductions ranged from about 24% to 65% depending on the climatic zone [43]. In the present analysis, the configuration with a diameter of 0.2 m and a length of 100 m yields design heating coil capacity reductions of 72% in Naples and 64% in Budapest, and cooling coil capacity reductions of 46.4% and 76.8%, respectively. These values are at the upper end, or slightly above, the range reported by D'Agostino et al., which is reasonable because the present work focuses on design-day peak loads in two climates

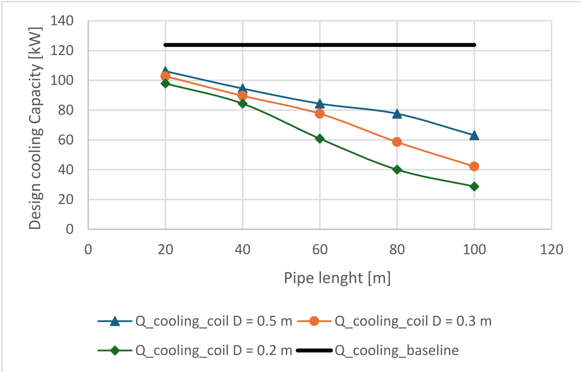

Fig. 16. Variation of the design cooling coil thermal capacity with EAHE in Budapest.

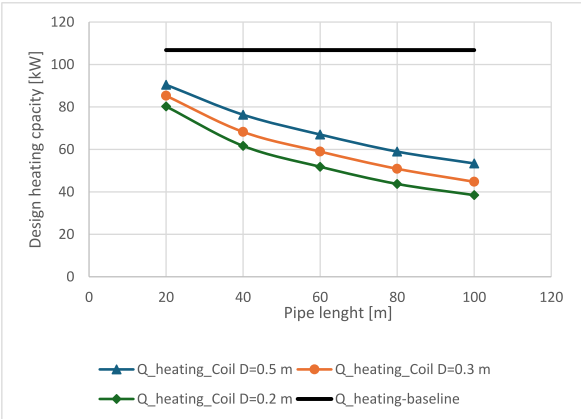

Fig. 17. Variation of the design heating coil thermal capacity with EAHE in Budapest.

Table 6
Design capacity of the heating coil using EAHE with diameter of 0.5 m and air velocity of 0.38 m/s in winter for Naples, considering various EAHE pipe lengths.

n°	EAHE pipe length	Point	T	Φ	ω	h	$Q_{heating\ coil}$
		[−]	[°C]	[%]	[g/kg]	[kJ/kg]	[kW]
1	20 m	E	5.6	43.6	2.4	11.8	53.0
		A	20.0	16.9	2.4	26.3	
		S	20.0	43.4	6.4	36.3	
2	40 m	E	8.5	35.7	2.4	14.7	42.3
		A	20.0	16.9	2.4	26.3	
		S	20.0	43.4	6.4	36.3	
3	60 m	E	10.2	31.9	2.4	16.4	36.0
		A	20.0	16.9	2.4	26.3	
		S	20.0	43.4	6.4	36.3	
3	80 m	E	11.3	29.6	2.4	17.5	32.0
		A	20.0	16.9	2.4	26.3	
		S	20.0	43.4	6.4	36.3	
4	100 m	E	12.5	27.4	2.4	18.7	27.6
		A	20.0	16.9	2.4	26.3	
		S	20.0	43.4	6.4	36.3	

characterized by pronounced air–soil temperature differences, whereas the cited study referred to multiple locations.

A similar behaviour is also observed when these findings are compared with annual simulations and monitoring studies. Zhang et al. evaluated an EAHE-assisted ventilation system in a hot-summer and cold-winter Chinese climate and reported seasonal reductions of approximately 16% in cooling energy demand and 50% in heating demand for ventilation air, with maximum pre-cooling and pre-heating temperature differences of about 20–21 °C for a pipe length of 100 m [30]. These values are consistent with the

Table 7
Design capacity of the heating coil using EAHE with diameter of 0.5 m and air velocity of 0.38 m/s in winter for Budapest, considering various EAHE pipe lengths.

n°	EAHE pipe length	Point	T	Φ	ω	h	$Q_{heating\ coil}$
		[−]	[°C]	[%]	[g/kg]	[kJ/kg]	[kW]
1	20 m	E	−4.6	46.1	1.2	−1.62	90.5
		A	20.0	8.5	1.2	23.2	
		S	20.0	43.4	6.4	36.3	
2	40 m	E	−0.8	31.9	1.2	3.4	76.3
		A	20.0	8.5	1.2	23.2	
		S	20.0	43.4	6.4	36.3	
3	60 m	E	1.7	28.8	1.2	4.8	67.0
		A	20.0	8.5	1.2	23.2	
		S	20.0	43.4	6.4	36.3	
3	80 m	E	3.9	24.6	1.2	7.0	59.0
		A	20.0	8.5	1.2	23.2	
		S	20.0	43.4	6.4	36.3	
4	100 m	E	5.5	22.1	1.2	8.6	53.4
		A	20.0	8.5	1.2	23.2	
		S	20.0	43.4	6.4	36.3	

Table 8
Design capacity of the heating coil using EAHE with diameter of 0.3 m and velocity of 1.06 m/s in winter for Naples, considering various EAHE pipe lengths.

n°	EAHE pipe length	Point	T	Φ	ω	h	$Q_{heating\ coil}$
		[−]	[°C]	[%]	[g/kg]	[kJ/kg]	[kW]
1	20 m	E	6.5	41.0	2.4	12.7	49.7
		A	20.0	16.9	2.4	26.3	
		S	20.0	43.4	6.4	36.3	
2	40 m	E	9.8	32.7	2.4	16.0	37.5
		A	20.0	16.9	2.4	26.3	
		S	20.0	43.4	6.4	36.3	
3	60 m	E	11.6	29.0	2.4	17.8	30.9
		A	20.0	16.9	2.4	26.3	
		S	20.0	43.4	6.4	36.3	
3	80 m	E	12.9	26.6	2.4	19.1	26.1
		A	20.0	16.9	2.4	26.3	
		S	20.0	43.4	6.4	36.3	
4	100 m	E	14.0	24.8	2.4	20.3	22.1
		A	20.0	16.9	2.4	26.3	
		S	20.0	43.4	6.4	36.3	

Table 9
Design capacity of the heating coil using EAHE with diameter of 0.3 m and air velocity of 1.06 m/s in winter for Budapest, considering various EAHE pipe lengths.

n°	EAHE pipe length	Point	T	Φ	ω	h	$Q_{heating\ coil}$
		[−]	[°C]	[%]	[g/kg]	[kJ/kg]	[kW]
1	20 m	E	−3.2	41.5	1.2	−0.2	85.3
		A	20.0	8.5	1.2	23.2	
		S	20.0	43.4	6.4	36.3	
2	40 m	E	1.4	27.1	1.2	5.7	68.3
		A	20.0	8.5	1.2	23.2	
		S	20.0	43.4	6.4	36.3	
3	60 m	E	3.9	24.6	1.2	7.0	59.0
		A	20.0	8.5	1.2	23.2	
		S	20.0	43.4	6.4	36.3	
3	80 m	E	6.1	21.1	1.2	9.3	50.9
		A	20.0	8.5	1.2	23.2	
		S	20.0	43.4	6.4	36.3	
4	100 m	E	7.8	18.8	1.2	10.9	44.8
		A	20.0	8.5	1.2	23.2	
		S	20.0	43.4	6.4	36.3	

Table 10
Design capacity of the heating coil using EAHE with diameter of 0.2 m and air velocity of 2.38 m/s in winter for Naples, considering various EAHE pipe lengths.

n°	EAHE pipe length	Point	T	Φ	ω	h	$Q_{heating\ coil}$
		[–]	[°C]	[%]	[g/kg]	[kJ/kg]	[kW]
1	20 m	E	7.5	38.2	2.4	13.7	46.0
		A	20.0	16.9	2.4	26.3	
		S	20.0	43.4	6.4	36.3	
2	40 m	E	11.3	29.6	2.4	17.5	32.0
		A	20.0	16.9	2.4	26.3	
		S	20.0	43.4	6.4	36.3	
3	60 m	E	13.3	26.0	2.4	19.5	24.6
		A	20.0	16.9	2.4	26.3	
		S	20.0	43.4	6.4	36.3	
3	80 m	E	14.3	24.3	2.4	20.6	21.0
		A	20.0	16.9	2.4	26.3	
		S	20.0	43.4	6.4	36.3	
4	100 m	E	15.2	23.0	2.4	21.5	17.7
		A	20.0	16.9	2.4	26.3	
		S	20.0	43.4	6.4	36.3	

Table 11
Design capacity of heating coil using EAHE with diameter of 0.2 m and air velocity of 2.38 m/s in winter for Budapest, considering various EAHE pipe lengths.

n°	EAHE pipe length	Point	T	Φ	ω	h	$Q_{heating\ coil}$
		[–]	[°C]	[%]	[g/kg]	[kJ/kg]	[kW]
1	20 m	E	−1.9	37.4	1.2	1.2	80.2
		A	20.0	8.5	1.2	23.2	
		S	20.0	43.4	6.4	36.3	
2	40 m	E	3.2	23.7	1.2	7.6	61.7
		A	20.0	8.5	1.2	23.2	
		S	20.0	43.4	6.4	36.3	
3	60 m	E	5.9	21.5	1.2	9.0	51.8
		A	20.0	8.5	1.2	23.2	
		S	20.0	43.4	6.4	36.3	
3	80 m	E	8.1	18.5	1.2	11.2	43.7
		A	20.0	8.5	1.2	23.2	
		S	20.0	43.4	6.4	36.3	
4	100 m	E	9.5	16.8	1.2	12.7	38.5
		A	20.0	8.5	1.2	23.2	
		S	20.0	43.4	6.4	36.3	

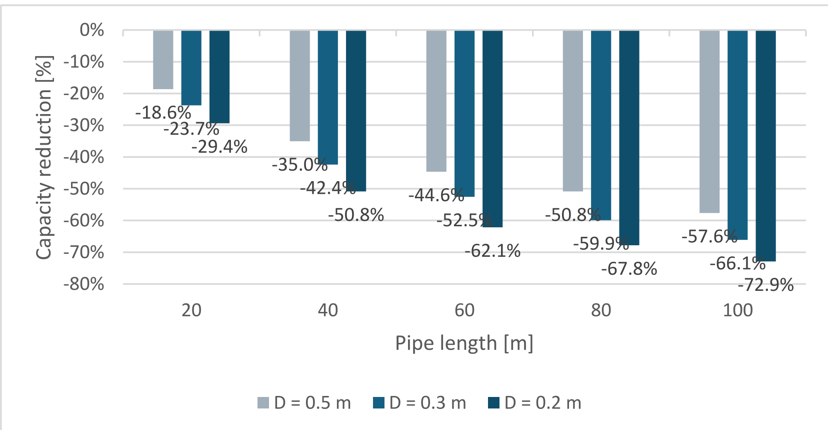

Fig. 18. Heating coil design capacity reduction using EAHE in Naples.

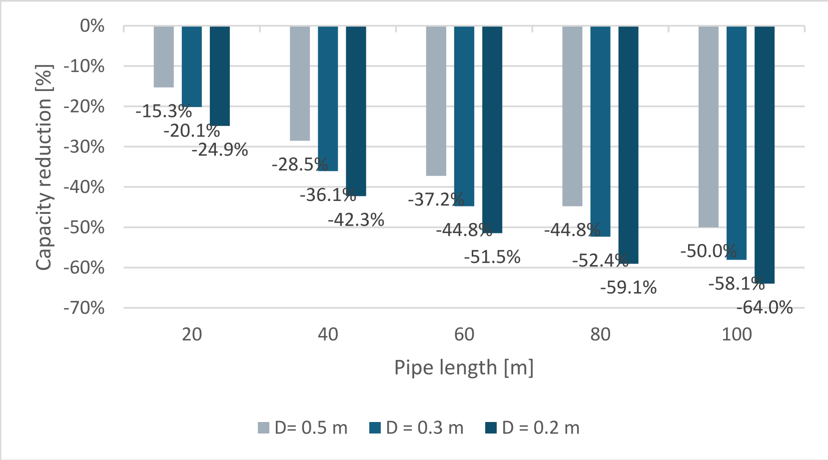

Fig. 19. Heating coil design capacity reduction using EAHE in Budapest.

Table 12
Design capacity of the cooling coil using EAHE with diameter of 0.5 m and air velocity of 0.38 m/s in summer for Naples, considering various EAHE pipe lengths.

n°	EAHE pipe length	Point	T	Φ	ω	h	$Q_{cooling\ coil}$
		[−]	[°C]	[%]	[g/kg]	[kJ/kg]	[kW]
1	20 m	E	28.3	61.3	14.8	66.1	117.5
		A	11.9	100	8.7	33.9	
		S	13.0	92.9	8.7	35.0	
2	40 m	E	25.6	71.6	14.8	63.4	107.5
		A	11.9	100	8.7	33.9	
		S	13.0	92.9	8.7	35.0	
3	60 m	E	23.9	79.3	14.8	61.6	101.1
		A	11.9	100	8.7	33.9	
		S	13.0	92.9	8.7	35.0	
3	80 m	E	22.3	87.3	14.8	60.0	95.1
		A	11.9	100	8.7	33.9	
		S	13.0	92.9	8.7	35.0	
4	100 m	E	21.3	92.8	14.8	58.9	91.3
		A	11.9	100	8.7	33.9	
		S	13.0	92.9	8.7	35.0	

Table 13
Design capacity of cooling coil using EAHE with diameter of 0.5 m and air velocity of 0.38 m/s in summer for Budapest, considering various EAHE pipe lengths.

n°	EAHE pipe length	Point	T	Φ	ω	h	$Q_{cooling\ coil}$
		[−]	[°C]	[%]	[g/kg]	[kJ/kg]	[kW]
1	20 m	E	27.3	61.2	13.9	63.0	106.1
		A	11.9	100	8.7	33.9	
		S	13.0	92.9	8.7	35.0	
2	40 m	E	24.2	73.5	13.9	59.8	94.5
		A	11.9	100	8.7	33.9	
		S	13.0	92.9	8.7	35.0	
3	60 m	E	21.5	86.6	13.9	57.0	84.4
		A	11.9	100	8.7	33.9	
		S	13.0	92.9	8.7	35.0	
3	80 m	E	19.7	96.7	13.9	55.2	77.6
		A	11.9	100	8.7	33.9	
		S	13.0	92.9	8.7	35.0	
4	100 m	E	18.1	100	13.0	51.2	63.1
		A	11.9	100	8.7	33.9	
		S	13.0	92.9	8.7	35.0	

Table 14
Design capacity of cooling coil using EAHE with diameter of 0.3 m and air velocity of 1.06 m/n in summer for Naples, considering various EAHE pipe lengths.

n°	EAHE pipe length	Point	T	Φ	ω	h	$Q_{cooling\ coil}$
		[−]	[°C]	[%]	[g/kg]	[kJ/kg]	[kW]
1	20 m	E	27.4	64.6	14.8	65.2	114.1
		A	11.9	100	8.7	33.9	
		S	13.0	92.9	8.7	35.0	
2	40 m	E	24.0	78.8	14.8	61.7	101.5
		A	11.9	100	8.7	33.9	
		S	13.0	92.9	8.7	35.0	
3	60 m	E	22.0	88.9	14.8	59.7	94.0
		A	11.9	100	8.7	33.9	
		S	13.0	92.9	8.7	35.0	
3	80 m	E	20.5	97.5	14.8	58.1	88.3
		A	11.9	100	8.7	33.9	
		S	13.0	92.9	8.7	35.0	
4	100 m	E	19.6	100	14.3	56.0	80.8
		A	11.9	100	8.7	33.9	
		S	13.0	92.9	8.7	35.0	

Table 15
Design capacity of cooling coil using EAHE with diameter of 0.3 and air velocity of 1.06 m/n in summer for Budapest, considering various EAHE pipe lengths.

n°	EAHE pipe length	Point	T	Φ	ω	h	$Q_{cooling\ coil}$
		[−]	[°C]	[%]	[g/kg]	[kJ/kg]	[kW]
1	20 m	E	26.4	64.5	13.9	62.1	102.8
		A	11.9	100	8.7	33.9	
		S	13.0	92.9	8.7	35.0	
2	40 m	E	22.9	79.5	13.9	58.5	89.6
		A	11.9	100	8.7	33.9	
		S	13.0	92.9	8.7	35.0	
3	60 m	E	19.7	96.7	13.9	55.2	77.6
		A	11.9	100	8.7	33.9	
		S	13.0	92.9	8.7	35.0	
3	80 m	E	17.7	100	13.9	49.9	58.6
		A	11.9	100	8.7	33.9	
		S	13.0	92.9	8.7	35.0	
4	100 m	E	16.2	100	13.0	45.4	42.2
		A	11.9	100	8.7	33.9	
		S	13.0	92.9	8.7	35.0	

Table 16
Design capacity of cooling coil using EAHE with diameter of 0.2 m and air velocity of 2.38 m/s in summer for Naples, considering various EAHE pipe lengths.

n°	EAHE pipe length	Point	T	Φ	ω	h	$Q_{cooling\ coil}$
		[−]	[°C]	[%]	[g/kg]	[kJ/kg]	[kW]
1	20 m	E	26.6	67.7	14.8	64.4	111.1
		A	11.9	100	8.7	33.9	
		S	13.0	92.9	8.7	35.0	
2	40 m	E	23.2	82.7	14.8	60.9	98.5
		A	11.9	100	8.7	33.9	
		S	13.0	92.9	8.7	35.0	
3	60 m	E	21.0	94.5	14.8	58.6	90.2
		A	11.9	100	8.7	33.9	
		S	13.0	92.9	8.7	35.0	
3	80 m	E	19.6	100	14.3	56.0	80.8
		A	11.9	100	8.7	33.9	
		S	13.0	92.9	8.7	35.0	
4	100 m	E	18.7	100	13.5	53.1	70.1
		A	11.9	100	8.7	33.9	
		S	13.0	92.9	8.7	35.0	

Table 17
Design capacity of cooling coil using EAHE with diameter of 0.2 m and air velocity of 2.38 m/s in summer for Budapest, considering various EAHE pipe lengths.

n°	EAHE pipe length	Point	T	Φ	ω	H	$Q_{cooling\ coil}$
		[−]	[°C]	[%]	[g/kg]	[kJ/kg]	[kW]
1	20 m	E	25.1	69.7	13.9	60.7	97.9
		A	11.9	100	8.7	33.9	
		S	13.0	92.9	8.7	35.0	
2	40 m	E	21.5	86.6	13.9	57.0	84.4
		A	11.9	100	8.7	33.9	
		S	13.0	92.9	8.7	35.0	
3	60 m	E	17.9	100	12.9	50.6	60.8
		A	11.9	100	8.7	33.9	
		S	13.0	92.9	8.7	35.0	
3	80 m	E	16.0	100	11.4	44.8	40.0
		A	11.9	100	8.7	33.9	
		S	13.0	92.9	8.7	35.0	
4	100 m	E	14.9	100	10.6	41.7	28.7
		A	11.9	100	8.7	33.9	
		S	13.0	92.9	8.7	35.0	

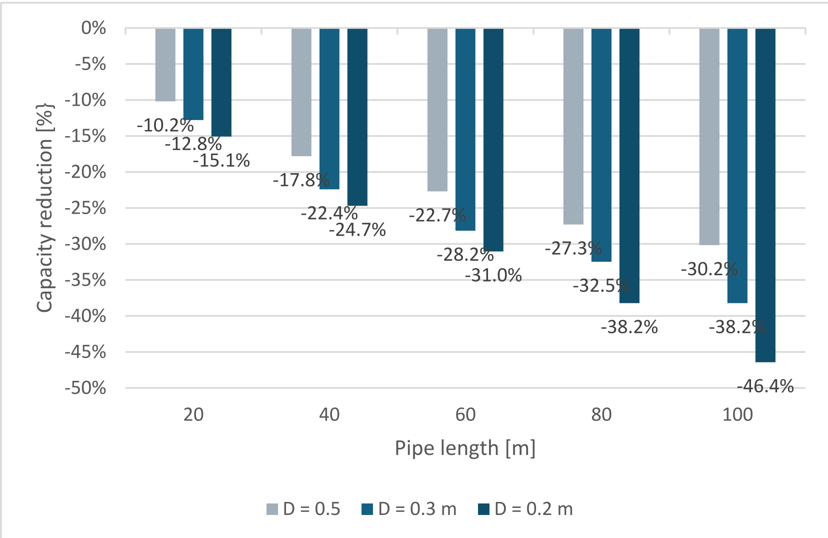

Fig. 20. Cooling coil design capacity reduction using EAHE in Naples.

inlet–outlet temperature variations predicted in this study for long, small-diameter pipes. On the experimental side, Hsu et al. monitored an EAHE system serving a restaurant in Taiwan and obtained an annual COP of around 27 for an installation with several 50 m pipes in parallel [54]. This is close to the COP of 30.5 and 42.4 found in the present study for the Budapest case. The higher efficiencies observed in our study can be attributed to the favourable air–soil temperature gradient, and to the fact that COP is evaluated at design operating conditions without accounting for part-load operation or auxiliary plant energy consumption.

Further considerations are that, according to Hungarian regulations, the operating period for a heating system is established from 15th September until 15th of May, with a restricted duration of 10 h per day, while for Naples is from Mid-November to the end of March with 10 h per day. The outcomes evident that although the reduction of design heating coil capacity is higher in Naples (72.9%) compared to Budapest (64%), the small reduction in Continental climate is considered highly significant due to the long operational period of heating system, supposing a consequent higher energy consumption. Further, based on the climatic characteristics, the operative period for the cooling system for Naples is defined from the beginning of June to the end of July, with a duration of 6 h per day and for the same period, with only 4 h per day, for Budapest. The study showed that the results of the cooling coil design capacity reduction are more pronounced for Budapest (76.8%); however, considering the extended operational duration of the system throughout the cooling season in Naples, the capacity reduction in cooling coil (46.6%) holds greater significance.

4.2. Investment and maintenance cost assessment

Table 18 reports the details about the investment costs of the EAHE field for all pipe geometries investigated. Across the 15

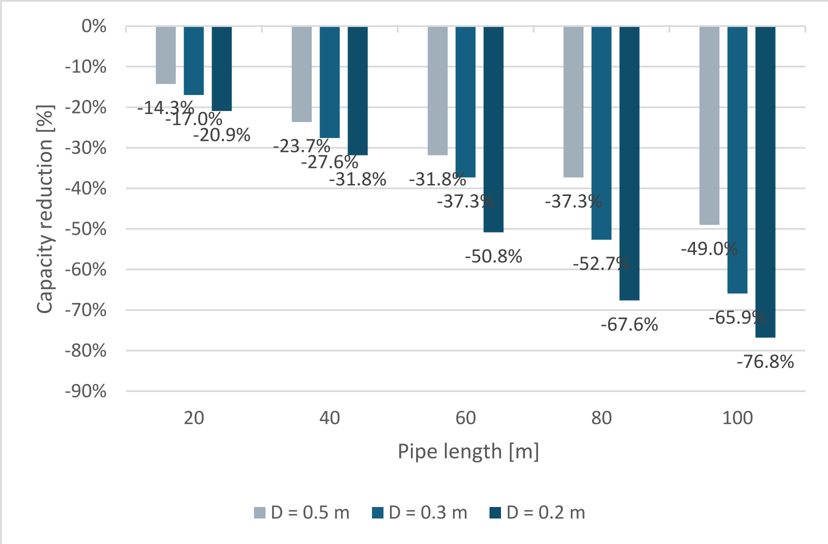

Fig. 21. Cooling coil design capacity reduction using EAHE in Budapest.

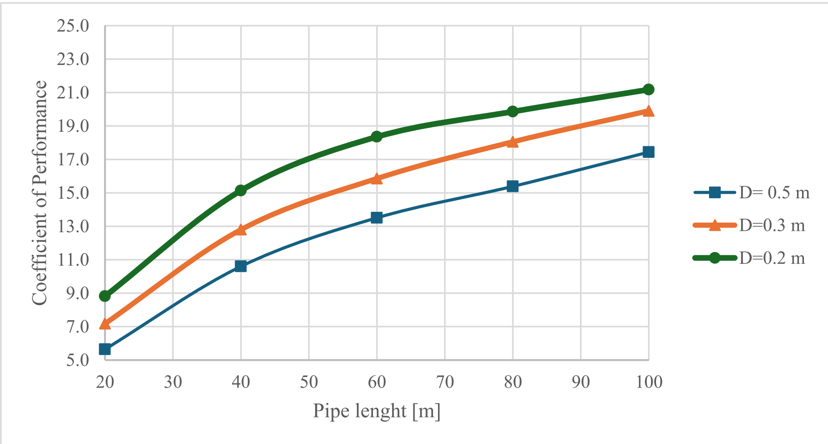

Fig. 22. COP of the hybrid EAHE–AHU system for different EAHE pipe lengths and diameters in Naples for winter.

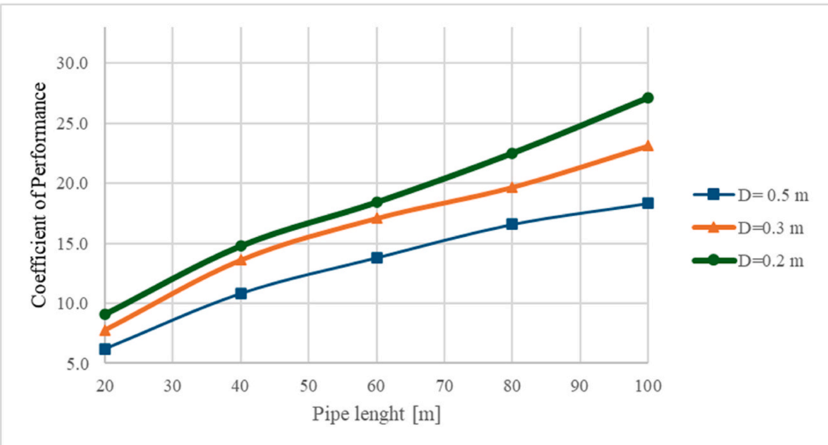

Fig. 23. COP of the hybrid EAHE–AHU system for different EAHE pipe lengths and diameters in Naples for summer.

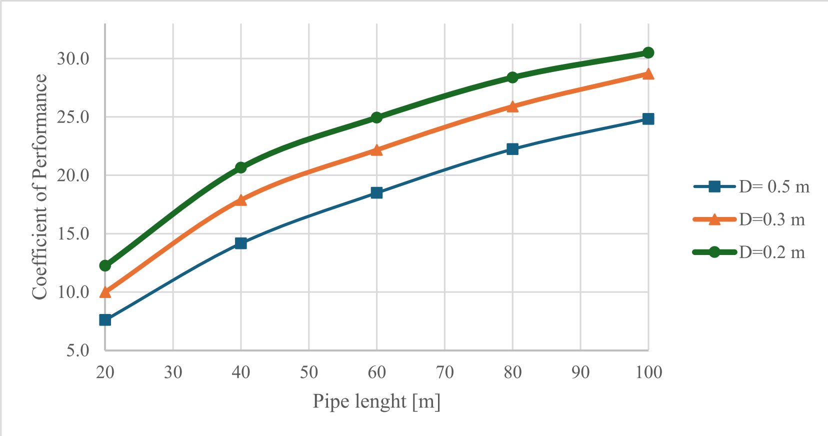

Fig. 24. COP of the hybrid EAHE–AHU system for different EAHE pipe lengths and diameters in Budapest for winter.

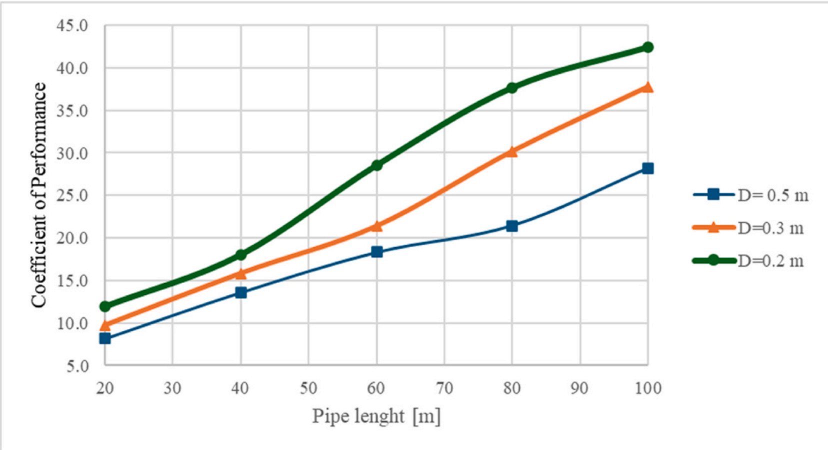

Fig. 25. COP of the hybrid EAHE–AHU system for different EAHE pipe lengths and diameters in Budapest for summer.

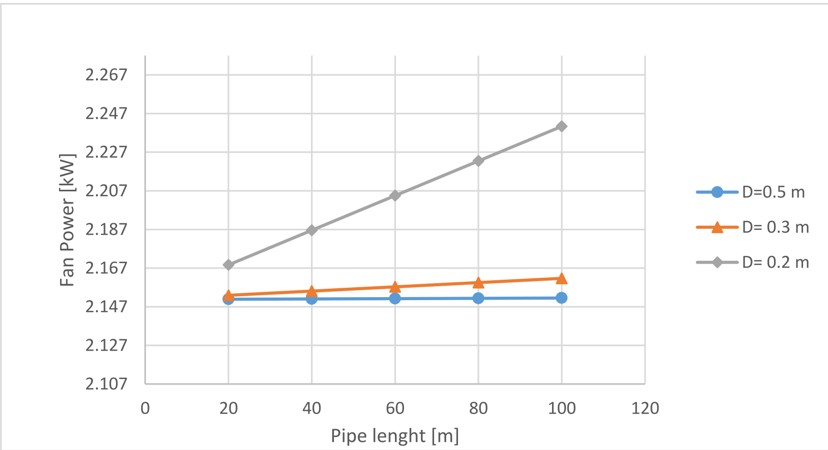

Fig. 26. Variation of fan power when using different pipe diameters and lengths.

Table 18
Details about the investment costs of the EAHE system for all investigated pipe geometries.

EAHE configuration by diameter	Length	Total pipe length	Excavation volume	Pipe supply	Excavation	Refilling + compaction	Collectors and joints	Drainage and inspection	Total EAHE investment cost
	[m]	[m]	[m^3]	[EUR]	[EUR]	[EUR]	[EUR]	[EUR]	[EUR]
EAHE diameter of 0.5 m	20	800	1600	24,944	15,856	11,456	2494	2748	57,499
	40	1600	3200	49,888	31,712	22,912	4989	3497	112,997
	60	2400	4800	74,832	47,568	34,368	7483	4245	168,496
	80	3200	6400	99,776	63,424	45,824	9978	4993	223,995
	100	4000	8000	124,720	79,280	57,280	12,472	5742	279,494
EAHE diameter of 0.3 m	20	800	1230	10,032	12,189	8807	1003	2301	34,332
	40	1600	2460	20,064	24,379	17,614	2006	2602	66,665
	60	2400	3690	30,096	36,568	26,420	3010	2903	98,997
	80	3200	4920	40,128	48,757	35,227	4013	3204	131,329
	100	4000	6150	50,160	60,946	44,034	5016	3505	163,661
EAHE diameter of 0.2 m	20	800	1000	4416	9910	7160	442	2132	24,060
	40	1600	2000	8832	19,820	14,320	883	2265	46,120
	60	2400	3000	13,248	29,730	21,480	1325	2397	68,180
	80	3200	4000	17,664	39,640	28,640	1766	2530	90,240
	100	4000	5000	22,080	49,550	35,800	2208	2662	112,300

configurations, the total EAHE investment cost ranges from 24,060 EUR (D = 0.2 m, L = 20 m) to 279,494 EUR (D = 0.5 m, L = 100 m). For each diameter, the total investment cost increases approximately linearly with pipe length, with an average increment per additional 20 m of about 22,060 EUR (D = 0.2 m), 32,330 EUR (D = 0.3 m) and 55,499 EUR (D = 0.5 m), consistent with the proportional growth of installed pipe length and trench volumes. At the maximum length (L = 100 m), the investment cost composition is diameter-dependent: for D = 0.2 m, excavation and refilling/compaction account for the largest shares (approximately 44% and 32%, respectively), whereas for D = 0.5 m the pipe procurement becomes the dominant component (approximately 45%) and excavation and refilling contribute a smaller fraction (about 28% and 21%, respectively).

Table 19 provides the 10-year maintenance costs for the investigated EAHE configurations. As reported in the methodology section 2.2, the maintenance cost is modelled as the sum of a fixed cost component and a variable component proportional to the total installed pipe length. Across the investigated EAHE geometries, the estimated 10-year maintenance cost ranges from 6300 EUR (D = 0.2 m, L = 20 m) up to 49,500 EUR (D = 0.5 m, L = 100 m).

Tables 20 and 21 quantify the avoided AHU coil investment costs associated with the coil downsizing enabled by the EAHE integration for Naples and Budapest, respectively. Over the investigated geometries, the total avoided coil investment cost ranges from 378 to 1606 EUR in Naples (Table 20) and 423-2092 EUR in Budapest (Table 21), increasing with pipe length and generally reaching the highest values for the configurations that induce the largest reductions in coil design capacity.

The investment cost assessment in Table 18 indicates that the relative importance of the cost components varies with pipe diameter and length. For smaller diameters, civil works (excavation and refilling/compaction) constitute the largest fraction of the total investment, so installation quantities and site-dependent construction conditions are expected to have a strong influence on total investment cost. As diameter increases, pipe procurement becomes progressively more significant, and for the largest diameter the pipe cost becomes comparable to, or larger than, the civil works contribution, highlighting the importance of diameter selection from an initial-cost perspective. In addition, the maintenance estimate (Table 19) indicates 10-year costs ranging from 6300 EUR to 49,500

Table 19
Details about the annual maintenance costs of the EAHE system for all investigated pipe geometries.

EAHE configuration by diameter	Length	Total pipe length	Fixed costs per 1 year	Fixed costs per 10 years	Pipe cleanout costs per 10 years	Total maintenance per 1 year	Total maintenance per 10 years
	[m]	[m]	[EUR]	[EUR]	[EUR]	[EUR]	[EUR]
EAHE diameter of 0.5 m	20	800	150	1500	9600	1110	11,100
	40	1600	150	1500	19,200	2070	20,700
	60	2400	150	1500	28,800	3030	30,300
	80	3200	150	1500	38,400	3990	39,900
	100	4000	150	1500	48,000	4950	49,500
EAHE diameter of 0.3 m	20	800	150	1500	6400	790	7900
	40	1600	150	1500	12,800	1430	14,300
	60	2400	150	1500	19,200	2070	20,700
	80	3200	150	1500	25,600	2710	27,100
	100	4000	150	1500	32,000	3350	33,500
EAHE diameter of 0.2 m	20	800	150	1500	4800	630	6300
	40	1600	150	1500	9600	1110	11,100
	60	2400	150	1500	14,400	1590	15,900
	80	3200	150	1500	19,200	2070	20,700
	100	4000	150	1500	24,000	2550	25,500

Table 20
Avoided AHU coil investment costs due to downsizing for all investigated EAHE geometries (Naples).

EAHE configuration by diameter	Length	Heating coil capacity (with EAHE)	Avoided heating-coil investment cost	Cooling coil capacity (with EAHE)	Avoided cooling-coil investment cost	Total avoided coil investment cost
	[m]	[kW]	[EUR]	[kW]	[EUR]	[EUR]
EAHE diameter of 0.5 m	20	53	186	117.5	192	378
	40	42.3	351	107.5	337	687
	60	36	448	101.1	429	877
	80	32	509	95.1	516	1025
	100	27.6	577	91.3	571	1147
EAHE diameter of 0.3 m	20	49.7	237	114.1	241	478
	40	37.5	424	101.5	423	848
	60	30.9	526	94	532	1058
	80	26.1	600	88.3	614	1214
	100	22.1	661	80.8	722	1384
EAHE diameter of 0.2 m	20	46	294	111.1	285	578
	40	32	509	98.5	467	976
	60	24.6	623	90.2	587	1209
	80	21	678	80.8	722	1401
	100	17.7	729	70.1	877	1606

Table 21
Avoided AHU coil investment costs due to downsizing for all investigated EAHE geometries (Budapest).

EAHE configuration by diameter	Length	Heating coil capacity (with EAHE)	Avoided heating-coil investment cost	Cooling coil capacity (with EAHE)	Avoided cooling-coil investment cost	Total avoided coil investment cost
	[m]	[kW]	[EUR]	[kW]	[EUR]	[EUR]
EAHE diameter of 0.5 m	20	90.5	153	106.1	270	423
	40	76.3	286	94.5	447	733
	60	67	373	84.4	601	974
	80	59	448	77.6	705	1153
	100	53.4	501	63.1	927	1427
EAHE diameter of 0.3 m	20	85.3	202	102.8	321	522
	40	68.3	361	89.6	522	883
	60	59	448	77.6	705	1153
	80	50.9	524	58.6	995	1519
	100	44.8	581	42.2	1246	1827
EAHE diameter of 0.2 m	20	80.2	249	97.9	395	645
	40	61.7	423	84.4	601	1024
	60	51.8	516	60.8	962	1477
	80	43.7	592	40	1279	1871
	100	38.5	640	28.7	1452	2092

EUR across the investigated geometries. The maintenance cost increases significantly with pipe length and diameter. For long and large-diameter configurations, the estimated annual maintenance expense becomes non-negligible compared with the corresponding initial investment. Therefore, it should be considered as an important constraint when selecting geometries for real applications.

When the investment and maintenance cost outcomes are interpreted together with the thermal results reported earlier, Tables 18–21 provide a practical basis for selecting geometry as a trade-off between thermal benefit (coil design capacity reduction) and initial investment. The avoided AHU coil investment cost reported in Tables 20 and 21 represents an evident credit directly linked to downsizing reductions; however, it remains small in absolute terms compared with the EAHE system investment and maintenance costs. Consequently, the economic relevance of the proposed configuration should be interpreted mainly in relation to the broader system-level benefits enabled by the EAHE integration (e.g., reduction of peak thermal demand, improvement of inlet air stability, reduction of annual energy expenditures), while a detailed assessment of operational savings is outside the scope of the present design and sizing study.

5. Conclusions

This study assessed the thermal performance of an Earth-to-Air Heat Exchanger (EAHE) integrated upstream of an Air Handling Unit (AHU) in a school building located in two distinct climatic contexts, Naples (Southern Italy, Köppen climate classification: Csa) and Budapest (Hungary, Dfb). The results demonstrate that the EAHE substantially enhances the pre-conditioning of outdoor air by exploiting the relative stability of ground temperature, which remains drastically higher than the outdoor air in winter and lower in summer. Therefore, the hybrid EAHE–AHU configuration significantly decreases the heating and cooling capacity required for the

AHU coils in both climates and definitively, although not evaluated in this study, the size of the heat generators.

The analysis confirms that the performance of the EAHE is strongly dependent on the geometric characteristics of the buried pipe. Smaller diameters increase air velocity and improve convective heat transfer, while longer pipes allow extended interaction with the surrounding soil. Among all examined configurations, the combination of a 0.2 m diameter and a 100 m length achieved the highest thermal effectiveness (approximately 88%), yielding the largest temperature variation between the EAHE inlet and outlet. In winter, this configuration reduced the design heating coil capacity by up to 64% in Budapest and 72.9% in Naples; similarly, in summer, the design cooling coil capacity was reduced by 76.8% and 46.4% in the two cities, respectively. These reductions confirm the significant contribution of EAHEs to decreasing peak design requirements.

A further analysis of the results shows several additional considerations of broader relevance. First, the EAHE does not serve only as a passive heat exchanger, but it effectively moderates the thermal variability of outdoor air by exploiting the nearly constant annual ground temperature. This stabilizing effect reduces the incidence of extreme thermal conditions at the AHU inlet and it has been shown that it significantly influences the sizing of downstream HVAC components (in particular heating and cooling coils). Furthermore, the system proves particularly advantageous in climates characterized by severe winters or pronounced seasonal fluctuations, as the temperature differential between air and soil is higher and the EAHE tends to operate more effectively. This indicates that the value of the EAHE integration in building-HVAC systems extends beyond energy savings and may include enhanced operational resilience.

The findings of the research also highlight the presence of diminishing returns associated with pipe diameter reduction. Indeed, although smaller diameters improve heat transfer, they simultaneously increase pressure losses and the associated fan power. Thus, optimal EAHE design cannot be determined solely by thermal effectiveness but should be based on a multi-parameter approach that balances heat exchange performance with ventilation energy requirements. Moreover, the occurrence of condensation within the pipe in summer, observed when the moist air reaches its dewpoint, introduces a shift from purely sensible to combined sensible–latent heat transfer. This effect affects cooling performance and suggests that EAHEs may also provide a degree of passive dehumidification under favourable conditions.

Lastly, an investment and maintenance cost assessment further investigated the practical feasibility of the EAHE geometries analysed in this study. The results showed that the initial investment and maintenance costs of the EAHE increase nearly linearly with pipe length and are influenced by pipe diameter due to procurement, deployment (excavations, refilling, compaction) and also pipe cleaning expenses. Also, the AHU coil downsizing enabled by the EAHE provides a not irrelevant but comparatively limited investment cost advantage, indicating that system geometry selection should be guided primarily by the targeted thermal benefit and by site-specific installation conditions.

5.1. Limitations

The present work has some limitations that should be acknowledged when interpreting the results. First, the analysis is carried out under steady-state design conditions for representative summer and winter days. Therefore, the reported reductions in heating and cooling coil capacity cannot be directly interpreted as annual energy savings.

In addition, the study focuses on thermal performance and does not investigate in detail the impact on the IAQ performance of aspects such as microbial growth, air filtration and condensate drainage effectiveness within the EAHE, which may be critical for real applications in school environments.

5.2. Future developments

Future research should focus on a more comprehensive evaluation of the energy savings provided by the EAHE–AHU system. These savings are not limited to the reduction of the heating and cooling coil capacity but also depend on the duration and frequency of the heating and cooling periods, which differ significantly between the two climatic contexts examined (Naples and Budapest). A detailed analysis of the seasonal operation could provide a more accurate estimation of the annual energy benefits of the hybrid system.

Moreover, in Mediterranean climates, it would be particularly valuable to assess whether the EAHE alone could maintain thermal comfort during certain periods of the year, potentially allowing for the complete bypass of the AHU, to determine if the passive pre-conditioning of the air provided by the EAHE allows, in addition to a satisfactory IAQ, also indoor thermal comfort without active intervention.

Long-term wet-surface effects (e.g., fouling/biofilm, changes in pressure drop and heat transfer) due to water vapor condensation inside the pipes in summer are not quantified in this design-day analysis and are therefore indicated as a future research/monitoring need.

Finally, a specific analysis would be useful to evaluate technical-economic indices, such as payback periods and net present value of the proposed configuration.

CRediT authorship contribution statement

D. D'Agostino: Writing – review & editing, Writing – original draft. **N. Kouki:** Writing – review & editing, Writing – original draft. **F. Minelli:** Writing – review & editing, Writing – original draft. **F. Minichiello:** Writing – review & editing, Writing – original draft. **A. Vityi:** Writing – review & editing, Writing – original draft.

Declaration of competing interest

The authors declare that they have no known competing financial interests or personal relationships that could have appeared to influence the work reported in this paper.

Acknowledgements

The professional part of this work was carried out within the framework of the project SMARS (SMARt and resilient Schools), financed by the University of Naples Federico II Research Funds (University Research Funding Program FRA 2024; CUP E63C24002430001).

This article was supported by the RRF-2.1.2-21-2022-00011 project, financed by the Government of Hungary within the framework of the Recovery and Resilience Facility.

Data availability

Data will be made available on request.

References

[1] International Energy Agency, Final Energy Consumption in the Buildings Sector, 2021. Paris, France, [Online]. Available: https://www.iea.org/data-and-statistics/charts/final-energy-consumption-in-the-buildings-sector-2021. (Accessed 24 November 2025).
[2] Department of Climate Change, Energy, the Environment and Water. Australian Government, HVAC Factsheet-Energy Breakdown, 2013 [Online]. Available: https://www.energy.gov.au/publications/hvac-factsheet-energy-breakdown#:~:text=A%20typical%20office%20building%20HVAC,other%20. (Accessed 24 November 2025).
[3] J. Castillo-González, F. Comino, F.J. Navas-Martos, M. Ruiz De Adana, Life cycle assessment of an experimental solar HVAC system and a conventional HVAC system, Energy Build. 256 (Feb. 2022) 111697, https://doi.org/10.1016/j.enbuild.2021.111697.
[4] F. Comino, J. Castillo González, F.J. Navas-Martos, M. Ruiz De Adana, Experimental energy performance assessment of a solar desiccant cooling system in southern Europe climates, Appl. Therm. Eng. 165 (Jan. 2020) 114579, https://doi.org/10.1016/j.applthermaleng.2019.114579.
[5] European Commission, Stepping up Europe's 2030 climate ambition investing in a climate-neutral future for the benefit of our people [Online]. Available: https://knowledge4policy.ec.europa.eu/publication/communication-com2020562-stepping-europe%E2%80%99s-2030-climate-ambition-investing-climate_en, Nov. 26, 2025.
[6] B.M. Ali, M. Akkaş, The green cooling factor: eco-innovative heating, ventilation, and air conditioning solutions in building design, Appl. Sci. 14 (1) (Dec. 2023) 195, https://doi.org/10.3390/app14010195.
[7] R. Maity, K. Sudhakar, A.A. Razak, Forestvoltaics, floatovoltaics and building applied photovoltaics (BAPV) potential for a university campus, Energy Eng 121 (9) (2024) 2331–2361, https://doi.org/10.32604/ee.2024.051576.
[8] P.A. Østergaard, N. Duic, Y. Noorollahi, S. Kalogirou, Renewable energy for sustainable development, Renew. Energy 199 (Nov. 2022) 1145–1152, https://doi.org/10.1016/j.renene.2022.09.065.
[9] D. D'Agostino, F. Minelli, F. Minichiello, HVAC system energy retrofit for a university lecture room considering private and public interests, Energies 18 (6) (Mar. 2025) 1526, https://doi.org/10.3390/en18061526.
[10] C. Fetting, THE EUROPEAN GREEN DEAL', *ESDN Off*, Vienna, Dec. 2020 [Online]. Available: chrome-extension://efaidnbmnnnibpcajpcglclefindmkaj/https://www.esdn.eu/fileadmin/ESDN_Reports/ESDN_Report_2_2020.pdf.
[11] N. Buckley, G. Mills, C. Reinhart, Z.M. Berzolla, Using urban building energy modelling (UBEM) to support the new european Union's green deal: case study of Dublin Ireland, Energy Build. 247 (Sep. 2021) 111115, https://doi.org/10.1016/j.enbuild.2021.111115.
[12] S. Charani Shandiz, B. Rismanchi, G. Foliente, Energy master planning for net-zero emission communities: state of the art and research challenges, Renew. Sustain. Energy Rev. 137 (Mar. 2021) 110600, https://doi.org/10.1016/j.rser.2020.110600.
[13] C. Harsito, R. Delfianti, F. Minelli, R.C. Syahroni, F. Nusyura, Thermoelectric system optimization for waste heat energy recovery in building kitchen hoods, Unconv. Resour. 8 (Oct. 2025) 100251, https://doi.org/10.1016/j.uncres.2025.100251.
[14] Y.-Y. Jing, H. Bai, J.-J. Wang, L. Liu, Life cycle assessment of a solar combined cooling heating and power system in different operation strategies, Appl. Energy 92 (Apr. 2012) 843–853, https://doi.org/10.1016/j.apenergy.2011.08.046.
[15] D. D'Agostino, M. Di Mascolo, F. Minelli, F. Minichiello, A new tailored approach to calculate the optimal number of outdoor air changes in school building HVAC systems in the Post-COVID-19 era, Energies 17 (11) (Jun. 2024) 2769, https://doi.org/10.3390/en17112769.
[16] M.I. Gomes, A.M. Barreiros, I. Pinto, A. Rodrigues, Improving indoor air quality in a higher-education institution through biophilic solutions, Sustainability 17 (11) (May 2025) 5041, https://doi.org/10.3390/su17115041.
[17] E. Bas (Ed.), Indoor Air Quality: Guide for Facility Managers, second ed., Fairmont Press, Lilburn, Ga New York, 2004.
[18] United States Environmental Protection Agency (EPA), Improving indoor air quality [Online]. Available: https://www.epa.gov/indoor-air-quality-iaq/improving-indoor-air-quality, Sep. 2025. (Accessed 18 November 2025).
[19] S. Ahmed, A. Ali, A. D'Angola, A review of renewable energy communities: concepts, scope, progress, challenges, and recommendations, Sustainability 16 (5) (Feb. 2024) 1749, https://doi.org/10.3390/su16051749.
[20] A.M. Elmalky, M.T. Araji, Optimization models for photosynthetic bioenergy generation in building façades, Renew. Energy 228 (Jul. 2024) 120607, https://doi.org/10.1016/j.renene.2024.120607.
[21] K.K. Jaiswal, et al., Renewable and sustainable clean energy development and impact on social, economic, and environmental health, Energy Nexus 7 (Sep. 2022) 100118, https://doi.org/10.1016/j.nexus.2022.100118.
[22] N. Kouki, A. Vityi, D. Belatrache, Exploring Earth air heat exchanger as an innovative and sustainable application for cooling and heating: excerpts from literature exploring Earth air heat exchanger as an innovative and sustainable application for cooling and heating: excerpts from literature, Waste Forum 3 (2025) 205–223.
[23] R. Di Filippo, O.S. Bursi, R. Di Maggio, Global warming and ozone depletion potentials caused by emissions from HFC and CFC banks due to structural damage, Energy Build. 273 (Oct. 2022) 112385, https://doi.org/10.1016/j.enbuild.2022.112385.
[24] J. Ríos-Arriola, et al., Air conditioning of an off-grid remote school with an Earth to air heat exchanger coupled indirectly to a solar cooling system, Int. J. Environ. Res. 18 (6) (Dec. 2024) 112, https://doi.org/10.1007/s41742-024-00662-x.
[25] L. Cirillo, A. Greco, C. Masselli, Computational investigation on daily, monthly and seasonal energy performances and economic impact through a detailed 2D FEM model of an earth to air heat exchanger coupled with an air conditioning system in a continental climate zone, Energy Build. 296 (Oct. 2023) 113365, https://doi.org/10.1016/j.enbuild.2023.113365.
[26] C. Dewangan, A.K. Shukla, R. Salhotra, A. Dewan, Analysis of an earth-to-air heat exchanger for enhanced residential thermal comfort, Environ. Prog. Sustain. Energy 43 (3) (May 2024) e14346, https://doi.org/10.1002/ep.14346.

[27] Q. Ma, G. Qian, M. Yu, L. Li, X. Wei, Performance of windcatchers in improving indoor air quality, thermal comfort, and energy efficiency: a review, Sustainability 16 (20) (Oct. 2024) 9039, https://doi.org/10.3390/su16209039.
[28] T.M. Abir Ahsan, Md S. Rahman, Md S. Ahamed, Geothermal energy application for greenhouse microclimate management: a review, Geothermics 127 (Mar. 2025) 103209, https://doi.org/10.1016/j.geothermics.2024.103209.
[29] S. Mohammadi, M.H. Jahangir, Numerical investigation of the saturating soil layers' effect on air temperature drops along the pipe of earth-air heat exchanger systems in heating applications, Geothermics 123 (Nov. 2024) 103109, https://doi.org/10.1016/j.geothermics.2024.103109.
[30] C. Zhang, J. Wang, L. Li, F. Wang, W. Gang, Utilization of earth-to-air heat exchanger to pre-Cool/Heat ventilation air and its annual energy performance evaluation: a case study, Sustainability 12 (20) (Oct. 2020) 8330, https://doi.org/10.3390/su12208330.
[31] Y. Yue, Z. Yan, P. Ni, F. Lei, G. Qin, Enhancing the performance of earth-air heat exchanger: a flexible multi-objective optimization framework, Appl. Therm. Eng. 244 (May 2024) 122718, https://doi.org/10.1016/j.applthermaleng.2024.122718.
[32] Z. Hu, Q. Yang, Y. Tao, L. Shi, J. Tu, Y. Wang, A review of ventilation and cooling systems for large-scale pig farms, Sustain. Cities Soc. 89 (Feb. 2023) 104372, https://doi.org/10.1016/j.scs.2022.104372.
[33] R.P. Castro, P. Dinho Da Silva, L.C.C. Pires, Advances in solutions to improve the energy performance of agricultural greenhouses: a comprehensive review, Appl. Sci. 14 (14) (Jul. 2024) 6158, https://doi.org/10.3390/app14146158.
[34] N. Kouki, D. D'Agostino, A. Vityi, Properties of earth-to-air heat exchangers (EAHE): insights and perspectives based on system performance, Energies 18 (7) (Apr. 2025) 1759, https://doi.org/10.3390/en18071759.
[35] F. Tasdelen, I. Dagtekin, A numerical study on heating performance of horizontal and vertical earth-air heat exchangers with equal pipe lengths, Therm. Sci. 26 (4 Part A) (2022) 2929–2939, https://doi.org/10.2298/TSCI2204929T.
[36] F.A. Lattieff, et al., Thermal analysis of horizontal earth-air heat exchangers in a subtropical climate: an experimental study, Front. Built Environ. 8 (Sep. 2022) 981946, https://doi.org/10.3389/fbuil.2022.981946.
[37] Z. Zhang, J. Sun, Z. Zhang, X. Jia, Y. Liu, Numerical research and parametric study on the thermal performance of a vertical earth-to-air heat exchanger system, Math. Probl Eng. 2021 (Jul. 2021) 1–16, https://doi.org/10.1155/2021/5557280.
[38] K. Huang, et al., Experimental and numerical research on the thermal performance of a vertical earth-to-air heat exchanger system, Geothermics 125 (Jan. 2025) 103182, https://doi.org/10.1016/j.geothermics.2024.103182.
[39] M. Merdassi, M. Aouissi, Numerical simulation and comparative analysis of Earth air heat exchanger designs, Int. J. Heat Technol. 42 (6) (Dec. 2024) 2143–2156, https://doi.org/10.18280/ijht.420633.
[40] K. Dehina, A.M. Mokhtari, B. Souyri, Energy modelling of a new co-current coaxial earth – water to air- heat exchanger. Case study: heating of house in Biskra - algeria, Geothermics 87 (Sep. 2020) 101836, https://doi.org/10.1016/j.geothermics.2020.101836.
[41] Y. Boutera, et al., Evaluation of the earth-air heat exchanger's performance in improving the indoor conditions of an industrial poultry house using computational fluid dynamics verified with field tests, J. Clean. Prod. 434 (Jan. 2024) 140218, https://doi.org/10.1016/j.jclepro.2023.140218.
[42] Y. Boutera, N. Boultif, A. Rouag, C. Beldjani, N. Moummi, Performance of earth-air heat exchanger in cooling, heating, and reducing carbon emissions of an industrial poultry farm: a case study, Energy Sources, Part A Recovery, Util. Environ. Eff. 44 (4) (Dec. 2022) 9564–9583, https://doi.org/10.1080/15567036.2022.2132323.
[43] D. D'Agostino, A. Greco, C. Masselli, F. Minichiello, The employment of an earth-to-air heat exchanger as pre-treating unit of an air conditioning system for energy saving: a comparison among different worldwide climatic zones, Energy Build. 229 (Dec. 2020) 110517, https://doi.org/10.1016/j.enbuild.2020.110517.
[44] J.P. Harrouz, D. Al Assaad, M. Orabi, K. Ghali, D. Ouahrani, N. Ghaddar, Modeling and optimization of poultry house passive cooling strategies in semiarid climates, Int. J. Energy Res. 45 (15) (Dec. 2021) 20795–20811, https://doi.org/10.1002/er.7139.
[45] L. Cirillo, S. Gargiulo, A. Greco, C. Masselli, V. Orabona, L. Verneau, Air-recirculating earth-to-air heat exchangers for efficient HVAC: energy and environmental analysis in school and residential buildings, J. Build. Eng. 116 (Dec. 2025) 114403, https://doi.org/10.1016/j.jobe.2025.114403.
[46] D. D'Agostino, F. Esposito, A. Greco, C. Masselli, F. Minichiello, Parametric analysis on an earth-to-air heat exchanger employed in an air conditioning system, Energies 13 (11) (Jun. 2020) 2925, https://doi.org/10.3390/en13112925.
[47] H. Koshlak, A review of earth-air heat exchangers: from fundamental principles to hybrid systems with renewable energy integration, Energies 18 (5) (Feb. 2025) 1017, https://doi.org/10.3390/en18051017.
[48] A. Zajch, W.A. Gough, G. Yoon, Influence of daily temperature behavior on earth-air heat exchangers: a case study from Aichi, Japan, City Environ. Interact. 8 (Nov. 2020) 100054, https://doi.org/10.1016/j.cacint.2020.100054.
[49] T. Kusuda, P.R. Achenbach, Earth temperatures and thermal diffusivity at selected stations in the United States, ASHRAE Trans. 71 (Part 1) (1965). NBS-8972.
[50] American Society of Heating, Refrigerating and Air-Conditioning Engineers (ASHRAE), Handbook - Fundamentals, ASHRAE, Atlanta, GA, USA', 2017. SI).
[51] B.W. Olesen, Revision of ISO17772-1 and EN16798-1 Standards Dealing with Indoor Environmental Quality, May 2019 [Online]. Available: https://www.aivc.org/system/files/02-02-04%20Bjarne%20Olesen%20AIVC%20workshop%20ISO%2017772.pdf. (Accessed 22 October 2025).
[52] President of the Italian Republic, DPR 412/93, Regolamento Recante Norme per La Progettazione, L'Installazione, L'Esercizio E La Manutenzione Degli Impianti Termici Degli Edifici Ai Fini Del Contenimento Dei Consumi Di Energia, in Attuazione Dell'Art. 4, Comma 4, Della L. 9 Gennaio 1991, N. 10, 1993.
[53] Government of Hungary, 676/2023. (XII. 29.) Korm. Rendelet a Központi Fűtésről És melegvíz-szolgáltatásról (In Hungarian)-Government Decree 676/2023 (XII.29.) on Central Heating and hot-water Service, Magyar Közlöny (Hungarian Official Gazette), Dec. 29, 2023.
[54] C.-Y. Hsu, P.-C. Huang, J.-D. Liang, Y.-C. Chiang, S.-L. Chen, The in-situ experiment of earth-air heat exchanger for a cafeteria building in subtropical monsoon climate, Renew. Energy 157 (Sep. 2020) 741–753, https://doi.org/10.1016/j.renene.2020.05.009.